© 2022. Published by The Company of Biologists Ltd | Development (2022) 149, dev200534. doi:10.1242/dev.200534

STEM CELLS AND REGENERATION

RESEARCH ARTICLE

Csf1rb regulates definitive hematopoiesis in zebrafish

Yimei Dai[1,*], Shuting Wu[2,*], Canran Cao[1], Rongtao Xue[3], Xuefen Luo[2], Zilong Wen[2,4,‡] and Jin Xu[1,‡]

ABSTRACT

In vertebrates, hematopoietic stem and progenitor cells (HSPCs) are capable of self-renewal and continuously replenishing all mature blood lineages throughout life. However, the molecular signaling regulating the maintenance and expansion of HSPCs remains incompletely understood. Colony-stimulating factor 1 receptor (CSF1R) is believed to be the primary regulator for the myeloid lineage but not HSPC development. Here, we show a surprising role of Csf1rb, a zebrafish homolog of mammalian CSF1R, in preserving the HSPC pool by maintaining the proliferation of HSPCs. Deficiency of *csf1rb* leads to a reduction in both HSPCs and their differentiated progenies, including myeloid, lymphoid and erythroid cells at early developmental stages. Likewise, the absence of *csf1rb* conferred similar defects upon HSPCs and leukocytes in adulthood. Furthermore, adult hematopoietic cells from *csf1rb* mutants failed to repopulate immunodeficient zebrafish. Interestingly, loss-of-function and gain-of-function assays suggested that the canonical ligands for Csf1r in zebrafish, including Csf1a, Csf1b and Il34, were unlikely to be ligands of Csf1rb. Thus, our data indicate a previously unappreciated role of Csf1r in maintaining HSPCs, independently of known ligands.

KEY WORDS: Csf1r, Hematopoiesis, Hematopoietic stem and progenitor cells

INTRODUCTION

Hematopoietic stem/progenitor cells (HSPCs) are responsible for generating multiple blood cell lineages, including erythrocytes and leukocytes, during early development and adulthood (Jagannathan-Bogdan and Zon, 2013). With erythrocytes providing oxygen and leukocytes providing immune protection for the body, disruption of hematopoiesis leads to severe blood diseases such as leukemia (Hatzimichael and Tuthill, 2010). Transplantation of HSPCs to a recipient in order to restore the normal hematopoietic system of the patient is a promising potential therapy for hematological disorders (Kumar and Geiger, 2017). To date, various strategies have been applied to increase the expansion of HSPCs *in vivo* or *ex vivo*. These strategies include stimulation with cytokines or growth factors (Matsunaga et al., 1998; Wohrer et al., 2014), ectopic expression of transcription factors for HSPC maintenance and expansion (Amsellem et al., 2003), modulation of the metabolic state of HSPCs by chemical inhibitors (Huang et al., 2012; Perry et al., 2011), or generation of HSPCs by reprogramming endothelium cells (Lis et al., 2017). However, all of these strategies resulted in the limited expansion of HSPCs (Kumar and Geiger, 2017). Therefore, a more comprehensive understanding of the mechanisms underlying HSPC maintenance and expansion *in vivo* is required to improve therapeutic applications.

In mammals, HSPCs originate from endothelial cells in the aorta, gonads and mesonephros region (Boisset et al., 2010; Cumano et al., 2001), and they migrate to the fetal liver for expansion and maturation before finally colonizing the bone marrow and sustaining adult hematopoiesis (Kieusseian et al., 2012). To fulfill the intense demand of short-lived mature blood cells to support the normal function of different organs, HSPCs need to be highly active to replenish mature blood cells and at the same time preserve their own cell pool (Bowie et al., 2006). The maintenance and cell fates of HSPCs are tightly regulated by a complicated interplay of intrinsic and extrinsic signals (Wei and Frenette, 2018). Among these signals, cytokine/receptor pairs are essential for modulating HSPC behaviors related to multiple aspects, including proliferation, differentiation, survival and mobilization in their niche. For example, SCF (also known as KITLG)/KIT, TPO/MPL and CXCL4 (also known as PF4)/CXCR2 signaling are necessary for the survival and maintenance of HSPCs (Deshpande et al., 2013; Kimura et al., 1998; Matsunaga et al., 1998; Sinclair et al., 2016; Tan et al., 1990). CXCL12/CXCR4 signaling is known for its important role in retaining HSPCs in the bone marrow niche in adult mice (Broxmeyer et al., 2005). Other cytokines, such as insulin-like factor 2 and angiopoietin 1, have been reported to enhance the expansion of HSPCs (Arai et al., 2004; Zhang and Lodish, 2004). Despite the fact that several cytokines and receptors have been demonstrated to be pivotal in directing HSPCs behaviors and fates, the whole picture of cytokines/receptors in regulating HSPC maintenance and expansion remains obscure.

CSF1R, also known as macrophage colony-stimulating factor receptor (M-CSFR) or Fms, belongs to the class III tyrosine kinase receptor family (Heldin and Lennartsson, 2013). The role of CSF1R has been well studied in mammals with a major focus on its functions in myeloid cells, especially the differentiation, proliferation and survival of tissue-resident macrophages (Stanley and Chitu, 2014). The function of CSF1R in the macrophage lineage depends on its ligands CSF1 or IL34 (Zelante and Ricciardi-Castagnoli, 2012). IL34 is essential for the development of Langerhans cells in the epidermis and microglia in the brain (Wang and Colonna, 2014; Wang et al., 2012; Wu et al., 2018), whereas CSF1 is required for other tissue-resident macrophages (Wiktor-Jedrzejczak et al., 1982). Apart from myelopoiesis, CSF1R also participates in the regulation of embryonic lymphopoiesis, as *Csf1r* marks myeloid-primed B-cell progenitors (Zriwil et al., 2016) or lymph-myeloid progenitors (Böiers et al., 2013). Intriguingly, *Csf1r* is also expressed in HSPCs (Miyamoto et al., 2002), and

[1]Laboratory of Immunology & Regeneration, School of Medicine, South China University of Technology, Guangzhou 510006, China. [2]Division of Life Science, State Key Laboratory of Molecular Neuroscience and Center of Systems Biology and Human Health, the Hong Kong University of Science and Technology, Clear Water Bay, Kowloon, Hong Kong, People's Republic of China. [3]Department of Hematology, Nanfang Hospital, Southern Medical University, Guangzhou, Guangdong 510515, China. [4]Greater Bay Biomedical Innocenter, Shenzhen Bay Laboratory, Shenzhen Peking University–Hong Kong University of Science and Technology Medical Center, Shenzhen 518055, China.
*These authors contributed equally to this work

‡Authors for correspondence (zilong@ust.hk; xujin@scut.edu.cn)

Y.D., 0000-0003-4611-4022; S.W., 0000-0003-2264-7393; R.X., 0000-0001-7269-4708; Z.W., 0000-0002-4260-7682; J.X., 0000-0002-6840-1359

Received 18 January 2022; Accepted 7 July 2022

Development (2022) 149, dev200534. doi:10.1242/dev.200534

CSF1/CSF1R signaling instructs myeloid fate commitment from hematopoietic stem cells (HSCs) at the single-cell level (Mossadegh-Keller et al., 2016). PLX5622, a chemical inhibitor that is presumed to target CSF1R, displays long-term suppressive effects on CD117 (KIT)$^{+}$ hematopoietic progenitors and CD34^{+} HSCs in mice (Lei et al., 2020). However, a recent study has indicated that the *Csf1r* expression in mouse HSPCs may be attributed to an artefact caused by association of macrophage remnants (Millard et al., 2021). Accordingly, CSF1R signal is undetectable in HSPCs in the bone marrow of CSF1R reporter mice (Grabert et al., 2020). The kinase dead mutation or hypomorphic mutation of *Csf1r* causes no defects on HSPCs (Rojo et al., 2019; Stables et al., 2022). These inconsistent findings suggest that further study is required to clarify the role of CSF1R in HSPC regulation.

Zebrafish is emerging as a powerful model for studying hematopoiesis with the advantages of external development, transparent embryos and easy genetic manipulation. Like mammals, zebrafish contains all mature blood cell types (Davidson and Zon, 2004). Initiating at around 30 h post-fertilization (hpf), HSPCs are generated via the endothelial-to-hematopoietic transition (EHT) process in the ventral wall of the dorsal aorta (VDA) and posterior blood island (Kissa and Herbomel, 2010; Tian et al., 2017). From 2 days post-fertilization (dpf) onwards, VDA-derived HSPCs migrate to caudal hematopoietic tissue (CHT), the equivalent hematopoietic tissue of mammalian fetal liver, for expansion and differentiation. Then, they populate the thymus and kidney after 3 dpf and 4 dpf, respectively. Similar to the bone marrow in mammals, zebrafish kidneys function as the major adult hematopoietic organ (Jin et al., 2007; Murayama et al., 2006). Apart from the similar ontogeny and cellular development of hematopoietic cells, molecular signals that regulate hematopoiesis are largely conserved between zebrafish and mammals (Perlin et al., 2017; Zhang et al., 2013). As a result of genome duplication in teleost fish, *Csf1r* has two orthologs in zebrafish: *csf1ra* and *csf1rb* (Braasch et al., 2006). Csf1ra is essential for microglial colonization in the brain and the development of xanthophore cells (Parichy et al., 2000; Wu et al., 2018; Herbomel et al., 2001). Csf1ra and Csf1rb work together as the functional homolog of mammalian CSF1R in regulating microglia development and distribution in the brain (Oosterhof et al., 2019, 2018). In addition, these two receptors also participate in the regulation of osteoclast cell activity during skeleton formation (Caetano-Lopes et al., 2020). Recently, Ferrero et al. found that *csf1rb* mutant zebrafish with a splice site mutation predominantly showed myeloid and B-lineage defects (Ferrero et al., 2020). However, the role of Csf1ra/Csf1rb in regulating hematopoiesis at a higher hierarchy has not yet been identified.

In the present study, we propose an unexpected role of Csf1rb in regulating HSPCs in zebrafish. *csf1rb*, but not *csf1ra*, was detected in HSPCs. Loss of function of Csf1rb, but not of Csf1ra, led to impaired maintenance of HSPCs during both early developmental stages and adult hematopoiesis. Consequently, this caused multiple mature blood-lineage defects. Surprisingly, the hematopoietic effects of Csf1rb did not rely on any of the dedicated ligands, including Csf1a, Csf1b and Il34, suggesting the existence of additional, as-yet-unknown signals for HSPC development.

RESULTS

csf1rb but not *csf1ra* is highly enriched in hemogenic endothelium and HSPCs at embryonic stages

To explore the role of Csf1r during early hematopoiesis in zebrafish, we determined the expression pattern of two zebrafish *CSF1R* orthologs, *csf1ra* and *csf1rb*, at the embryonic stage. Consistent with previous reports, whole-mount *in situ* hybridization (WISH) showed that *csf1ra* was exclusively detected in *mpeg1*$^{+}$ macrophages and neural crest-derived xanthophores (Fig. S1D-F) (Herbomel et al., 2001; Ellett et al., 2011; Wu et al., 2018). Likewise, *csf1rb* was also detected in macrophages, but the number of *csf1rb*-positive cells was lower than that of *csf1ra*-positive cells (Fig. S1A-C). Surprisingly, *csf1rb* was also found to be expressed in non-macrophages in the VDA region at 2 dpf (Fig. S1B), and *csf1rb* but not *csf1ra* transcripts were highly enriched in the VDA region at 30-36 hpf (Fig. S1G), when definitive HSPCs began to emerge from hemogenic endothelium (HE) in the VDA (Kissa and Herbomel, 2010). This observation coincided with that reported by Ferrero et al. (2020). We suspected that *csf1rb* was expressed in the HE and newly formed HSPCs. Indeed, the co-staining analysis showed that *csf1rb* was co-expressed with the endothelium marker *flk1* (*kdrl*) and HSPC marker *cmyb* (*myb*) at 30-36 hpf (Fig. 1A,B) (Choi et al., 2007; Ellett et al., 2011; North et al., 2007). Consistent with this notion, a substantial portion of the *csf1rb*-positive cells in the VDA of 2 dpf embryos co-expressed the HSPC markers *cmyb* and *runx1* (Fig. 1C,D) (Bertrand et al., 2008; Gering and Patient, 2005; Lam et al., 2010; Zhang et al., 2011), but not *mpeg1* (Fig. S1B), although not all *cmyb*$^{+}$ or *runx1*$^{+}$ cells displayed *csf1rb* expression. Collectively, these data demonstrate that *csf1rb* is enriched in HE and HSPCs at the embryonic stages of zebrafish development. This conclusion was further supported by the observation that *csf1rb* expression was completely abolished in the VDA and CHT in *runx1*-deficient mutant fish (Fig. S1H), in which the formation of HSPCs was largely abrogated (Jin et al., 2009).

Csf1rb deficiency perturbs HSPC maintenance at embryonic stages

The enriched expression of *csf1rb* in HE and HSPCs implies that it may play an important role in the top hierarchy of definitive hematopoiesis. To address this question, we generated a *csf1rb*-deficient zebrafish mutant, *csf1rb*^{hkz15} (called *csf1rb* mutant in the following text; siblings referred to wild-type and heterozygous fish), with the CRISPR-Cas9 system. The mutant *csf1rb* genome harbored a 2333 bp fragment deletion from intron 9 to exon 13 (Fig. S2A), and the relative expression level of *csf1rb* in *csf1rb* mutants was much lower than that in siblings (Fig. S2B). To test whether loss of Csf1rb function would perturb HSPC formation, we first performed time-lapse imaging to track the process of EHT, during which the HE sprout from the aorta and turn into HSPCs (Kissa and Herbomel, 2010; Tian et al., 2017). To monitor and quantify the events of EHT, we utilized *Tg(flk1:NLS-Eos)* fish (Fukuhara et al., 2014), in which endothelial cells express the photo-convertible nuclear localization signal (NLS)-tagged Eos fluorescence protein (NLS-Eos). Upon UV light irradiation, Eos switches from green fluorescence to red fluorescence (Fig. 2A). At 28-30 hpf, we converted nine endothelial cells in the VDA (one per somite) in each embryo and followed their behaviors for approximately 26 h with time-lapse imaging (Fig. 2A, lower panels, Movies 1-2). The results showed that the budding number of converted endothelial cells was comparable between *csf1rb* mutants and siblings (3.3 cells versus 3.8 cells on average per fish) (Fig. 2B). Consistent with the results of time-lapse imaging, the expression of *cmyb,* a well-known HSPC marker (Bertrand et al., 2008; Xia et al., 2021; Xue et al., 2017; Zhang et al., 2011), in *csf1rb* mutants was similar to that in siblings from 30 hpf to 2 dpf (Fig. 2C-E). These data indicate that Csf1rb is not required for the specification and budding of HSPCs during early development.

Development (2022) 149, dev200534. doi:10.1242/dev.200534

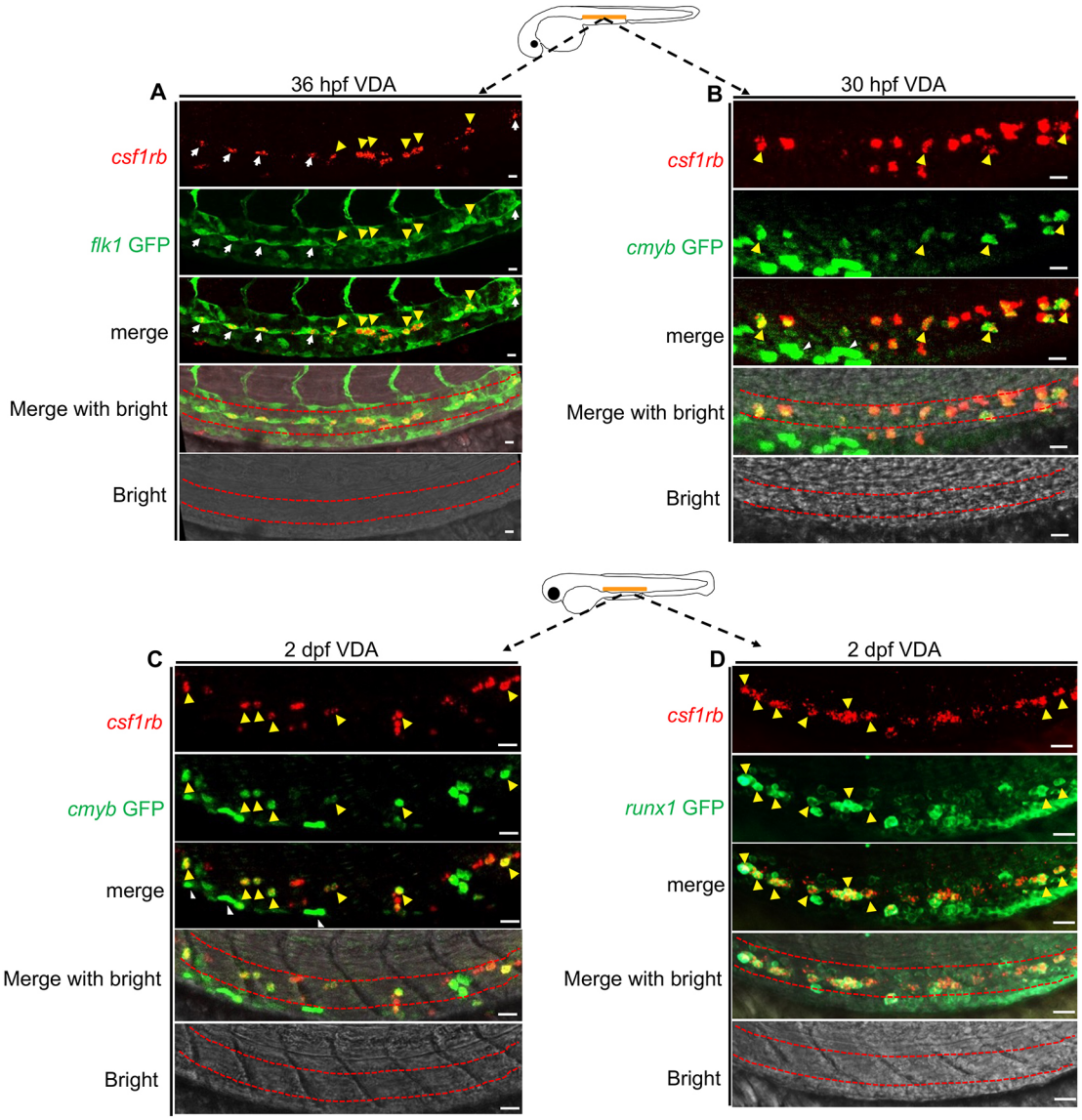

Fig. 1. *Csf1rb* is highly expressed in hemogenic endothelium and HSPCs. (A,B) Diagram at the top shows a 30-36 hpf zebrafish embryo; the orange line indicates the VDA region. (A) WISH of *csf1rb* in the *Tg(flk1*:*GFP)* line at 36 hpf in the VDA region. White arrows indicate colocalization of *csf1rb* (red) and GFP$^+$ HE (green) with a flat shape. Yellow arrowheads indicate *csf1rb*-positive naïve HSPCs with a round shape. *n*=12. (B) WISH of *csf1rb* in the *Tg(cmyb:GFP)* line at 30 hpf in the VDA region. Yellow arrowheads indicate colocalization of *csf1rb* (red) and GFP$^+$ HSPCs (green). White arrowheads indicate *cmyb*-GFP$^+$ multiciliated cells. *n*=12. (C,D) Diagram at the top shows a 2 dpf zebrafish embryo; the orange line indicates the VDA region. (C) WISH of *csf1rb* in the VDA of *Tg(cmyb:GFP)* at 2 dpf. White arrowheads indicate *cmyb*-GFP$^+$ multiciliated cells. *n*=12. (D) WISH of *csf1rb* in the VDA of *Tg(runx1*:en-GFP*)* at 2 dpf. Yellow arrowheads indicate colocalization of *csf1rb* (red) and GFP$^+$ HSPCs (green). *n*=15. Brightfield images are two to five layers stacked to show the VDA region (indicated by the red dashed lines). Scale bars: 20 µm.

However, as the mutant fish developed to 3 dpf, when most of the HSPCs accumulate in the CHT (Jin et al., 2007), the number of *cmyb*$^+$ cells in the CHT region was severely reduced (Fig. 2F,G). Consistent with this, another HSPC-enriched marker, *runx1* (Gering and Patient, 2005; Tamplin et al., 2015; Xue et al., 2017), also displayed a similar reduction in *csf1rb* mutants (Fig. 2H,I). To confirm the HSPC defects in *csf1rb* mutants, we further checked *cmyb*$^+$ *pu.1* (*spi1b*)$^-$ cells (non-myeloid HSPCs) in *csf1rb* siblings and mutants within the *Tg(cmyb:GFP)* line (North et al., 2007), to exclude the possibility that the reduction of *cmyb*$^+$ cells in *csf1rb* mutants could be attributed to myeloid cell defects (Ferrero et al., 2020). Our results showed that a significant portion of *cmyb*-GFP positive cells were *pu.1* negative, and not only *pu.1*$^+$ cells (myeloid cells) but also *cmyb*$^+$*pu.1*$^-$ cells (non-myeloid HSPCs) showed a significant decrease in *csf1rb* mutants (Fig. S3A-D). We also examined downstream blood cell markers in *csf1rb* mutants at 5-6 dpf. Unlike primitive erythrocytes, which only retain AE1-globin protein but decrease *αe1-globin* (*hbae1.1*) RNA in the cell, and mainly exist in the circulation, definitive erythrocytes maintain *αe1-globin* RNA expression and locate in the CHT at 5 dpf (Fig. S4) (Jin et al., 2009). We found that not only *αe1-globin* but also *βe2-globin* (*hbbe2*) (Ganis et al., 2012) and Gata1 (Monteiro et al., 2011) were reduced in *csf1rb* mutants at 5-6 dpf (Fig. 2J,K, Fig. S3E-H), suggesting defects in definitive HSPC-derived erythroid cells. We also observed a substantial reduction of Lcp1$^+$ myeloid cells (Meijer et al., 2008) and *lck*$^+$/*rag1*$^+$ T cells (Langenau et al., 2004) in *csf1rb* mutants at 5 dpf (Fig. 2L-O, Fig. S3I-J). Considering T cells at early larval stages are mixed origins from

Development (2022) 149, dev200534. doi:10.1242/dev.200534

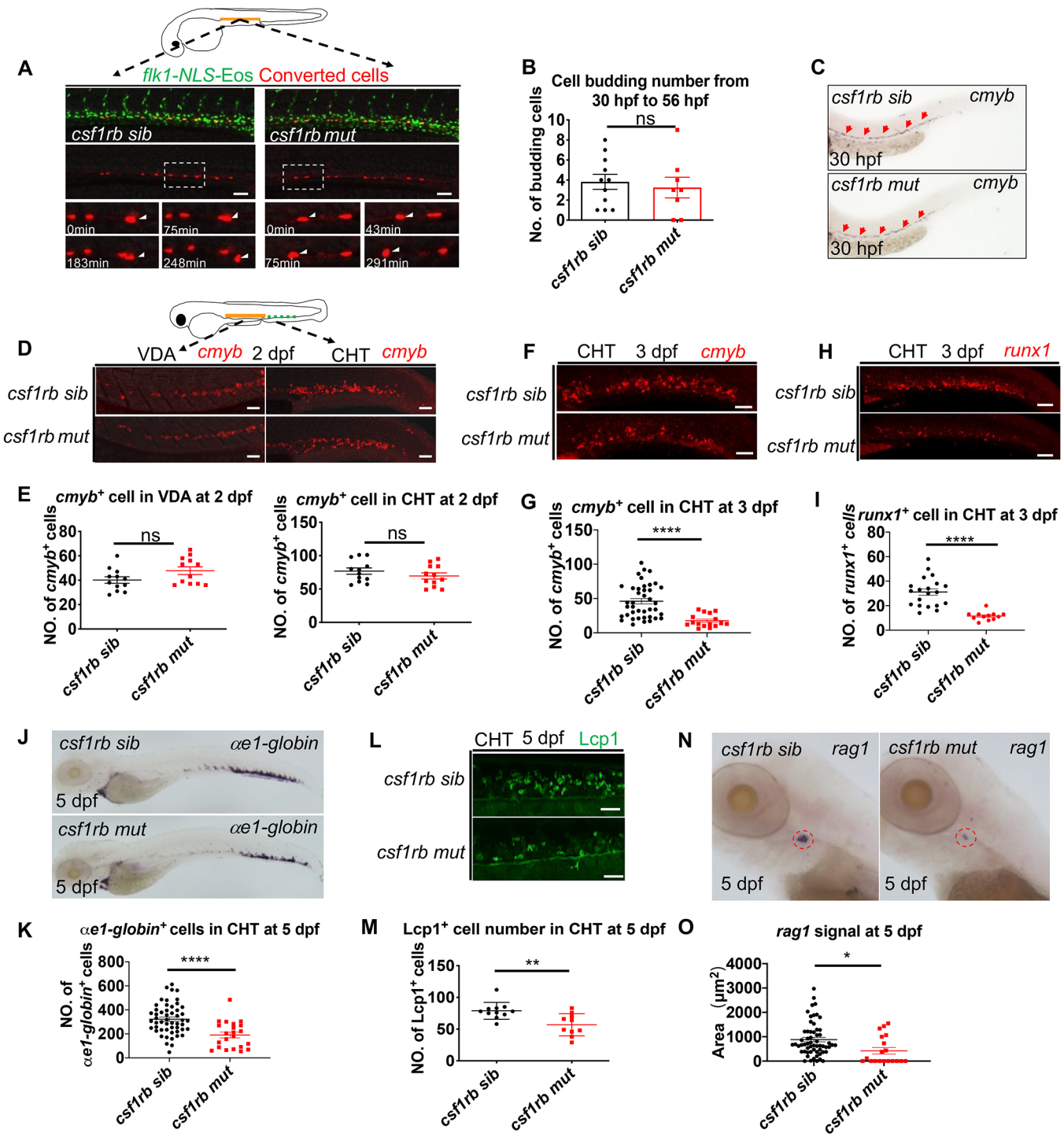

Fig. 2. *csf1rb* deficiency does not interfere with the formation of HSPCs but leads to HSPC reduction and multiple lineage defects at early developmental stages. (A) Budding behavior of the converted cell in the VDA in siblings (sib) and *csf1rb* mutants (mut). Orange line in the diagram indicates the VDA region. Upper panels show *flk1*-NLS-Eos^{+} green endothelial cells in the VDA; nine cells were converted into red after UV light conversion. Lower panels show the budding behavior of the cell in the white dashed line, enlarged at different time points in the bottom panels and indicated by white arrowheads. The time scale is shown in the left corner. (B) Quantification of the number of cells budding among converted endothelial cells over 26 h in siblings (n=11) and *csf1rb* mutants (n=8). (C) WISH of *cmyb* in siblings (n=16) and *csf1rb* mutants (n=16) at 30 hpf; red arrows show naïve HSPC signal in the VDA. (D) WISH of *cmyb* in siblings and *csf1rb* mutants at 2 dpf. (E) Quantification of *cmyb*$^{+}$ HSPCs in siblings (n=12) and *csf1rb* mutants (n=12) in the VDA and the CHT at 2 dpf. (F) WISH of *cmyb* in *csf1rb* mutants and siblings at 3 dpf. (G) Quantification of *cmyb*$^{+}$ HSPCs in siblings (n=40) and *csf1rb* mutants (n=16) in the CHT at 3 dpf. (H) WISH of *runx1* in siblings and *csf1rb* mutants at 3 dpf. (I) Quantification of *runx1*$^{+}$ HSPCs in siblings (n=20) and *csf1rb* mutants (n=12) in the CHT at 3 dpf. (J) WISH of *αe1-globin* in siblings and *csf1rb* mutants at 5 dpf. (K) Quantification of *αe1-globin*$^{+}$ erythrocytes in siblings (n=52) and *csf1rb* mutants (n=22) in the CHT at 5 dpf. (L) Immunostaining of Lcp1 in the CHT at 5 dpf in siblings and *csf1rb* mutants. (M) Quantification of the Lcp1^{+} myeloid cells in siblings (n=11) and *csf1rb* mutant (n=10) embryos. (N) WISH of *rag1* at 5 dpf in siblings and *csf1rb* mutants; red dashed circle indicates the position of the thymus. (O) Quantification of the *rag1*$^{+}$ thymus area in siblings (n=59) and *csf1rb* mutant (n=19). Scale bars: 50 µm. Data are presented as mean±s.e.m. *P<0.05, **P<0.01, ****P<0.0001; ns, not significant.

Development (2022) 149, dev200534. doi:10.1242/dev.200534

both non-HSC progenitors and HSCs (Tian et al., 2017; Ulloa et al., 2021), we further checked T cells after 40 dpf, when T cells in the thymus are originated purely from HSCs (Tian et al., 2017). It has been demonstrated that a *coro1a*-driven reporter can mark T cells in the thymus region (He et al., 2020; Xue et al., 2021), and we found that the *coro1a*$^{+}$ thymus area in *csf1rb* mutants at 45 dpf was significantly smaller than that in siblings (Fig. S3K-M). These results suggest definitive hematopoiesis failure in *csf1rb* mutants. The HSPC defect was confirmed in the compound heterozygous mutants of *csf1rb* by crossing our *csf1rb* mutant with the published *csf1rb*^{re01} mutant (Fig. S5) (Oosterhof et al., 2018), demonstrating that the observed phenotypes were a consequence of *csf1rb* deficiency. Interestingly, the development of primitive myeloid and erythroid lineages was largely unaffected in *csf1rb* mutants (Fig. S6A-C), and primitive microglia only displayed a slight reduction (Fig. S6D and E), compared with a near-complete depletion of primitive microglia in *csf1ra* mutants (Oosterhof et al., 2018; Wu et al., 2018). These results suggest that, in contrast to the important role of Csf1ra in primitive myeloid cell development (Wu et al., 2018), Csf1rb appears to play a crucial role in definitive HSPC development. This conclusion was further supported by the findings that *csf1ra* deficiency had no obvious effect on HSPC development and *csf1ra/b* double deficiency did not cause a more severe HSPC phenotype (Fig. S7). Taken together, these data show that Csf1rb is essential for HSPC development at the early stages of zebrafish development.

Csf1rb regulates HSPC proliferation at embryonic stages

To examine the cellular basis underlying the defect of HSPCs in *csf1rb* mutants, a terminal deoxynucleotidyl transferase dUTP nick end labeling (TUNEL) assay was performed to monitor the death of HSPCs in the *Tg(cmyb:GFP);csf1rb* transgenic mutant line. TUNEL staining showed that there was no excessive death of *cmyb-GFP*$^{+}$ cells in *csf1rb* mutants (Fig. S8), suggesting that the reduction of HSPCs was not caused by apoptotic cell death. To support this argument further, we performed time-lapse imaging of the *Tg(cmyb:GFP);csf1rb* transgenic mutant line to trace the fate of *cmyb*-GFP^{+} HSPCs in the VDA and CHT from 2.5 dpf to 4 dpf, when *cmyb*$^{+}$ HSPCs were significantly lower in the mutant embryos (Fig. 2F,G). Consistent with the TUNEL assay results, time-lapse imaging revealed no excessive death of *cmyb*-GFP^{+} HSPCs in *csf1rb* mutants (Movies 3,4). These data indicate that the reduction of HSPCs in *csf1rb* mutants cannot be attributed to excessive cell death.

We therefore speculated that the reduction of HSPCs in *csf1rb* mutants could be due to a defect in cell proliferation. We performed a bromodeoxyuridine (BrdU) incorporation assay to examine the proliferation of HSPCs in the *Tg(cmyb:GFP);csf1rb* transgenic mutant line. The results showed that not only the *cmyb*-GFP^{+} HSPC number but also the percentage of BrdU^{+} proliferating HSPCs were significantly reduced in the CHT region of *csf1rb* mutants compared with that in siblings (Fig. 3, Fig. S9), demonstrating the important role of Csf1rb in regulating the expansion of HSPCs. Reporter lines driven by the *coro1a* promoter have been demonstrated to faithfully label HSPCs/hematopoietic cells in the VDA and CHT region at embryonic stages (Huang et al., 2019; Li et al., 2012); thus, we also utilized the *Tg(coro1a:kaede)* line to monitor the proliferation of *coro1a*$^{+}$ HSPCs/hematopoietic cells in the VDA region of *csf1rb* mutants, in which these cells could be converted from green to red by 405 nm UV light (Mizuno et al., 2003; Xu et al., 2016). Twenty to thirty *coro1a*$^{+}$ cells in the VDA were converted at about 2.5 dpf and their proliferation was traced for 20 h by time-lapse imaging (Fig. S10A,B). The results showed that the percentage of dividing *coro1a*$^{+}$ HSPCs/hematopoietic cells in the VDA of *csf1rb* mutants (35%) was significantly lower than that in siblings (52%) (Fig. S10C). Taken together, Csf1rb is essential for the expansion of HSPCs, and the absence of Csf1rb results in a severe reduction of HSPCs and their downstream blood lineages.

csf1rb-deficient adult fish suffer from attenuated HSPCs and leukopenia

As *csf1rb*-deficient mutants can survive to adulthood, we next investigated whether Csf1rb also plays a similar role in adult hematopoiesis. Blood cells were collected from the peripheral circulation and whole kidney marrow (WKM), the adult hematopoietic organ in zebrafish (Traver et al., 2003), from adult (3-8 months) *csf1rb* mutants and siblings and subjected to flow cytometry. We examined the blood lineages utilizing *Tg(globin:*

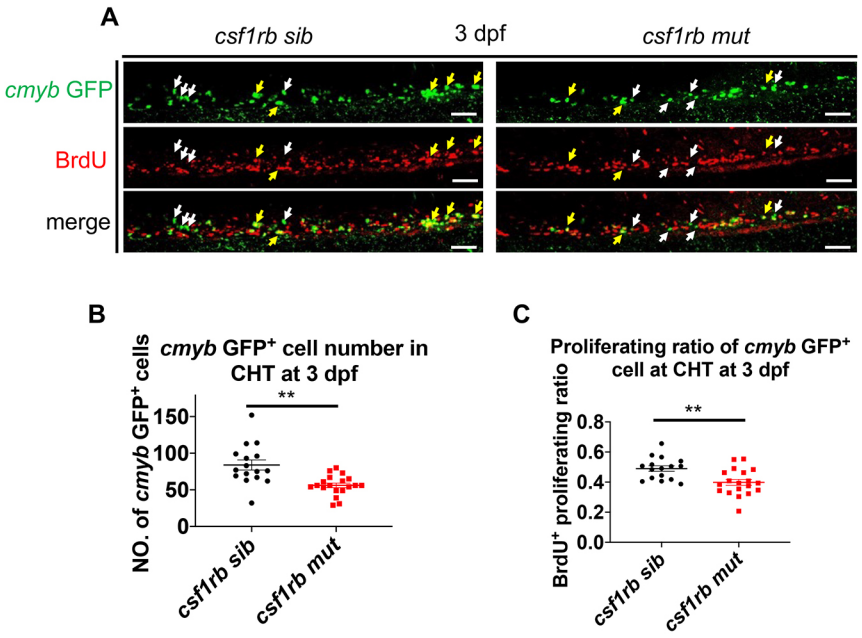

Fig. 3. *Csf1rb* deficiency impairs the proliferation capacity of HSPCs. (A) Immunostaining of *cmyb*-GFP (green) and BrdU (red) in the CHT at 3 dpf in siblings and *csf1rb* mutants after BrdU labeling for 1 h. Yellow arrows show BrdU^{+} HSPCs, white arrows indicate GFP single-positive HSPCs. Scale bars: 20 µm. (B) Quantification of *cmyb*-GFP^{+} HSPCs in the CHT at 3 dpf in siblings (n=16) and *csf1rb* mutants (n=19). (C) Quantification of the proliferation ratio of *cmyb*-GFP^{+} HSPCs in the CHT at 3 dpf in siblings (n=16) and *csf1rb* mutants (n=19). Data are presented as mean ±s.e.m. $^{**}P$<0.01.

Development (2022) 149, dev200534. doi:10.1242/dev.200534

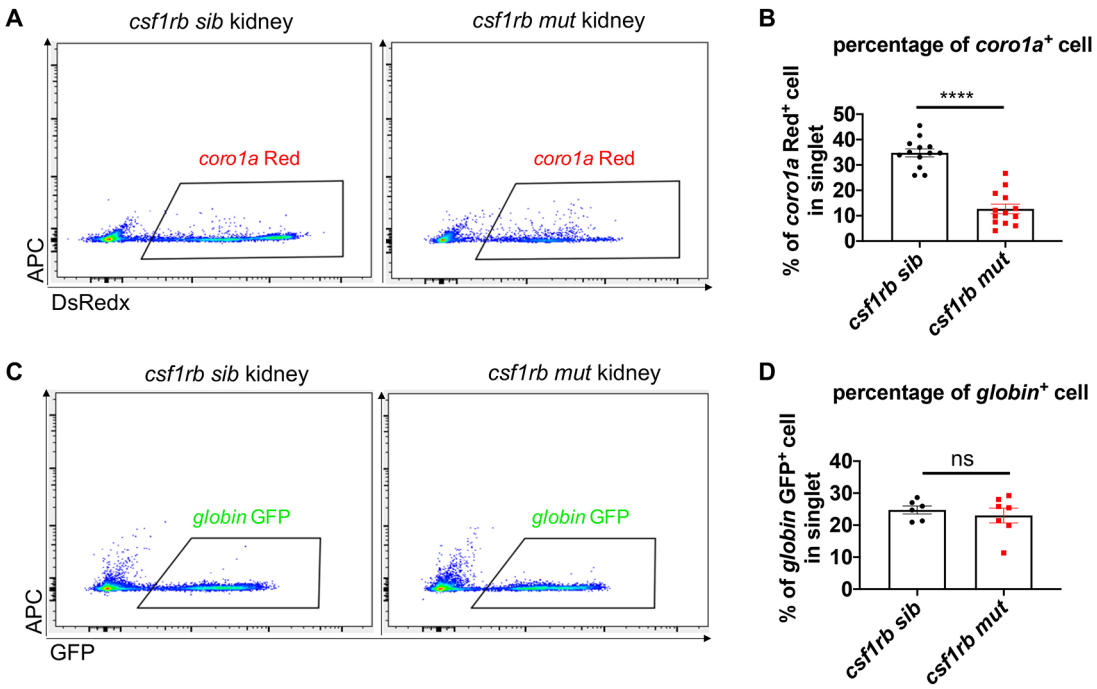

Fig. 4. Defective leukocytes/progenitors but not erythrocytes in *csf1rb* mutant at adulthood. (A) Flow cytometry analysis of *coro1a*-DsRedx$^+$ leukocytes/progenitors in the WKM of adult siblings and *csf1rb* mutants. (B) Percentage of *coro1a*$^+$ cells in singlets of the WKM in siblings (n=13) and *csf1rb* mutants (n=13). (C) Flow cytometry analysis of *globin*-GFP$^+$ erythrocytes in the WKM of adult siblings and *csf1rb* mutants. (D) Percentage of *globin*$^+$ cells in singlets of the WKM in siblings (n=6) and *csf1rb* mutants (n=7). Data are presented as mean±s.e.m. ****P<0.0001; ns, not significant.

GFP) and *Tg(coro1a:DsRedx)*, in which erythroid cells and leukocytes/progenitors, respectively, are labeled (Huang et al., 2019; Li et al., 2012; Tian et al., 2017). We found that the *coro1a*$^+$ cells in the WKM were significantly reduced in adults with *csf1rb* deficiency (12.7% of the WKM cells in mutants versus 34.8% in siblings) (Fig. 4A,B, Fig. S11A). By contrast, the percentage of the *globin*$^+$ erythroid cells in the WKM were comparable between *csf1rb* siblings and mutant (Fig. 4C,D, Fig. S11B). To confirm the normal erythrocyte population in adult *csf1rb* mutants, we took the same volume of peripheral blood from *csf1rb*-deficient adult fish and siblings to check the absolute cell number of *globin*-GFP$^+$ erythroid cells using flow cytometry (Figs S11C and S12A). As expected, the number of erythroid cells in circulation was normal in *csf1rb* mutant fish (Fig. S12B). We also examined the morphology of erythrocytes and found no difference between *csf1rb* mutants and siblings (Fig. S12C). All of these results suggested that the shortage of erythroid population at embryonic stages stemming from *csf1rb* deficiency can be compensated for and recover with the growth of zebrafish. To test this possibility further, we examined the blood lineages at earlier stages utilizing *Tg(globin:GFP)* and *Tg(coro1a:DsRedx)*. The results showed that in *csf1rb* mutant fish, the percentage and absolute cell number of *globin*$^+$ erythroid cells, but not *coro1a*$^+$ cells, recovered to the normal level at as early as 11 dpf (Figs S11D, S12D-G). *lck*$^+$ T lymphocytes (Tian et al., 2017) in the thymus remained defective in *csf1rb* mutants at 11 dpf (Fig. S12H).

To investigate further the HSPC defects in *csf1rb* mutant adult fish, we injected *pu.1* morpholino (MO) into *runx1* mutant embryos to deplete all hematopoiesis-derived immune cells and obtain immune-deficient embryos (Kissa and Herbomel, 2010; Rhodes et al., 2005; Fraint et al., 2020). We transplanted the same dosage of adult WKM cells (on average 400 cells per fish) from *csf1rb* mutants or siblings with *Tg(globin:GFP)* and *Tg(coro1a:DsRedx)* into immunodeficient embryos at 2 dpf and raised these fish into adults to determine the donor contribution of leukocytes and erythrocytes with the *globin*-GFP and *coro1a*-DsRedx reporters (Fig. 5A). We found that four out of 13 fish were reconstituted by *csf1rb* sibling donor-derived hematopoietic cells, as shown by the DsRedx$^+$ cells in the skin/kidney and GFP$^+$ erythroid cells in the circulation (Fig. 5B-E, Fig. S11A). However, none of the 24 fish transplanted with *csf1rb* mutant WKM cells was grafted by donor-derived blood cells (Fig. 5B-E, Fig. S11A), indicating the impaired repopulating ability of adult HSPCs in *csf1rb* mutant fish. These data suggest that Csf1rb deficiency also attenuates the hematopoietic capacity of adult HSPCs.

The canonical Csf1r ligands probably are not involved in HSPC maintenance

In mammals, CSF1 and IL34 serve as the ligands for CSF1R during the regulation of myeloid cell development (Stanley and Chitu, 2014). In zebrafish, the Il34-Csf1ra axis has been demonstrated to mediate microglia seeding in the brain (Kuil et al., 2019; Wu et al., 2018), and Csf1a/b-Csf1ra regulate xanthophore cell development and pattern melanocytes to direct stripe formation (Parichy and Turner, 2003; Patterson and Parichy, 2013; Wu et al., 2018). Recently, Il34 was reported to regulate granulopoiesis via Csf1rb (Hason et al., 2022). We wondered which ligand functioned via Csf1rb in regulating HSPC maintenance, so we examined the *cmyb*$^+$ HSPCs in *csf1a*, *csf1b* and *il34* mutant fish (Wu et al., 2018). However, no defects in HSPCs were observed in these ligand mutants (Fig. 6A,B). Considering possible compensation effects between these three ligands, the phenotypes of double mutants and triple mutants were examined. Similar to the single mutants, HSPCs were normal in all of the mutants (Fig. 6A,B). However, the *csf1a*$^{-/-}$ *csf1b*$^{-/-}$ fish fully recapitulated the pigmentation defects of *csf1ra*$^{-/-}$ mutant fish (Fig. S13A) (Parichy and Turner, 2003), indicating total loss of function of both ligand forms. *Il34* mutant fish have also been

Development (2022) 149, dev200534. doi:10.1242/dev.200534

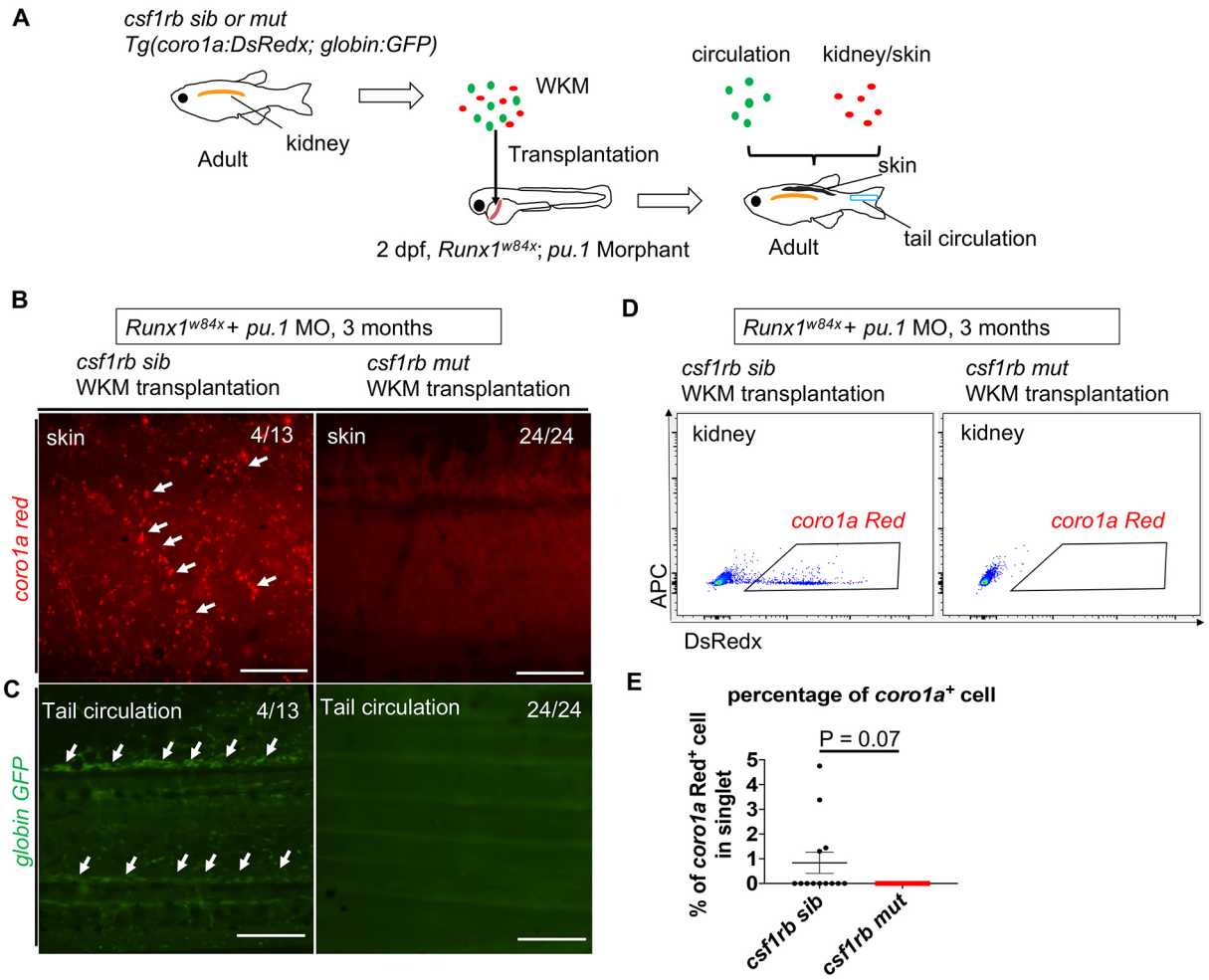

Fig. 5. Impaired engraftment ability of hematopoietic cells from adult WKM of *csf1rb*-deficient fish. (A) Work flow of WKM transplantation. Single-cell-stage embryos from the *runx1*^{w84x} mutant were injected with *pu.1* MO to create immunodeficient fish (*runx1*^{w84x}; *pu.1* morphant). The WKM cell suspension was prepared from *csf1rb* siblings and mutants with the *Tg(coro1a:DsRedx)* and *Tg(globin:GFP)* background and was transplanted into the vessel around the yolk of 2 dpf immunodeficient fish. These fish were raised to adults, and donor-derived blood cells were checked in the kidney, skin and circulation. Red circles indicate the *coro1a*-Red^{+} cells, green circles indicate the *globin*-GFP^{+} cells, the orange bar indicates the kidney, the black bar indicates the skin and the blue bar indicates the tail circulation. (B) *Coro1a*-Red^{+} cells on the skin of 3-month-old immunodeficient recipient fish after transplantation. Four out of 13 recipient fishes transplanted with WKM of sibling donor fishes were reconstituted by donor *coro1a*-Red^{+} cells on the skin (white arrows), but none of the 24 recipient fishes transplanted with WKM from *csf1rb* mutant donor fish had *coro1a*-Red^{+} cells on the skin. Scale bars: 200 µm. (C) *Globin*-GFP^{+} cells in the circulation in tails of 3-month-old immunodeficient recipient fish after transplantation. The four fish transplanted with WKM of sibling donors with *coro1a*-Red^{+} cells on the skin were also reconstituted by donor-derived red blood cells in the circulation (white arrows), and none of the fishes transplanted with WKM from *csf1rb* mutant donors had donor-derived *globin*-GFP^{+} cells in the circulation. Scale bars: 200 µm. (D) Flow cytometry analysis of WKM of 3-month-old immunodeficient recipient fish after transplantation. The four fish transplanted with WKM of sibling donors with *coro1a* Red^{+} cells on the skin were also reconstituted by donor-derived *coro1a*-Red^{+} cells in the kidney marrow, and none of the fishes transplanted with WKM of *csf1rb* mutant donors had donor-derived *coro1a*-Red^{+} cells in the kidney. (E) Percentage of *coro1a*$^{+}$ cells in the WKM of recipients transplanted with the WKM cells from *csf1rb* siblings (*n*=13) or mutants (*n*=24). Data are presented as mean±s.e.m.

demonstrated to have defective microglia (Wu et al., 2018). To test whether these ligands work as the ligand of Csf1rb, we overexpressed each ligand utilizing the *Tg(hsp70:csf1a)*, *Tg(hsp70:csf1b)* and *Tg(hsp70:il34)*, in which the expression of the ligand was activated after heat shock. The embryos were heat shocked at 2, 2.5 and 3 dpf for 1 h, respectively, and *cmyb*$^{+}$ HSPCs were evaluated at 3.5 or 4 dpf. The results showed that ectopic expression of *csf1a* or *csf1b* increased the population of xanthophore cells on the surface of the embryos (Fig. S13B,C), and overexpression of *il34* augmented macrophages in the embryos (Fig. S13D,E), demonstrating gain of function of these ligands after heat shock. However, we found that overexpression of Csf1a or Csf1b or Il34 was insufficient to boost HSPCs, although they could expand xanthophores and macrophages (Fig. 6C-E). In conclusion, the above data demonstrate that Csf1a, Csf1b and Il34, the canonical ligands for Csf1r in zebrafish, are not likely to be the ligands of Csf1rb in regulation of hematopoiesis.

DISCUSSION

In the present study, we provide the first genetic evidence to suggest that Csf1r can function at a higher hematopoietic hierarchy. We reveal a crucial role of Csf1rb in preserving the HSPC pool by maintaining the expansion of HSPCs at embryonic stages. We also found that Csf1rb regulates the reconstitution ability of adult HSPCs, which was attenuated by *csf1rb* deficiency. Interestingly, the impaired proliferation of HSPCs in *csf1rb*-deficient embryonic fish led to defects in multiple lineages, including erythrocytes,

Development (2022) 149, dev200534. doi:10.1242/dev.200534

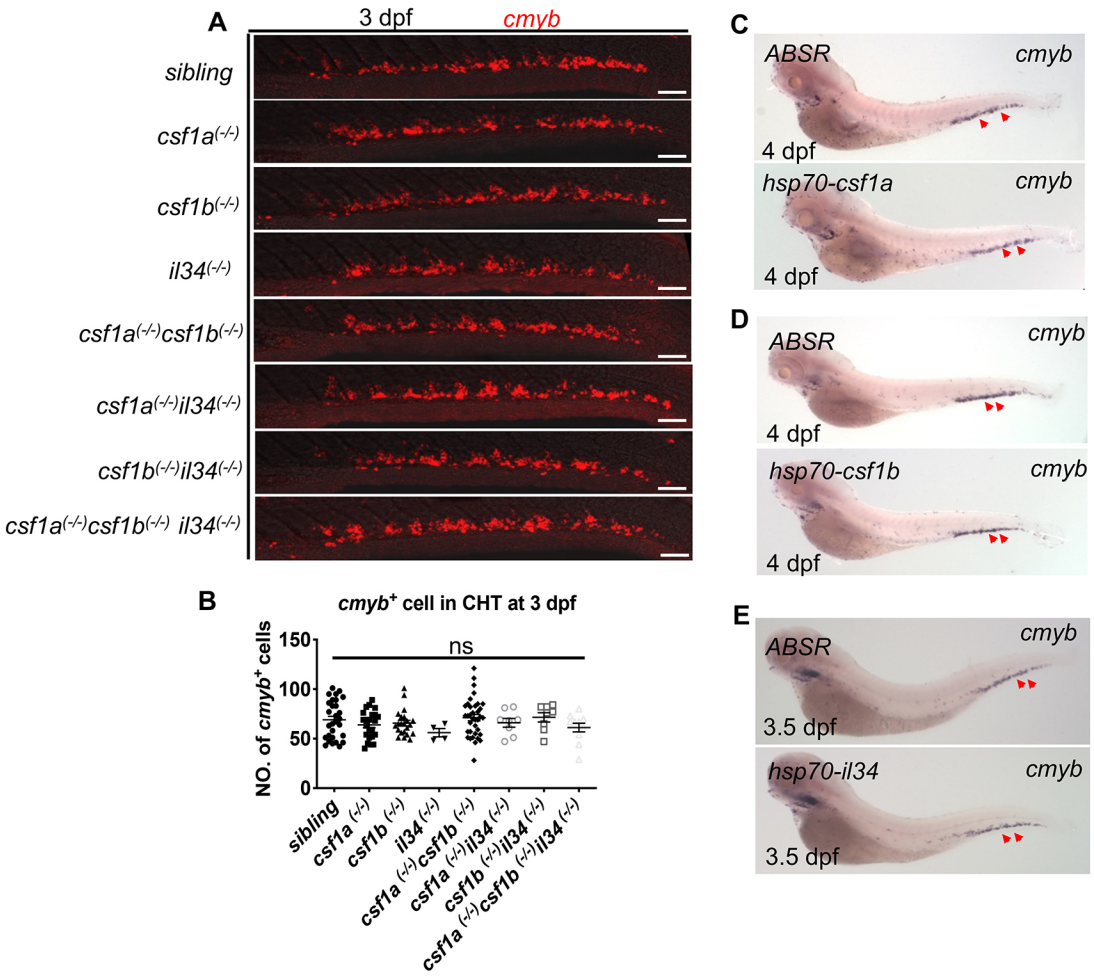

Fig. 6. Canonical ligands of Csf1r, including Csf1 and Il34, are neither required nor sufficient for HSPC expansion. (A) WISH of *cmyb* at 3 dpf in siblings and *csf1a*, *csf1b* and *il34* single, double and triple mutants. Scale bars: 50 µm. (B) Quantification of *cmyb*$^{+}$ HSPCs in CHT at 3 dpf in siblings and *csf1a*, *csf1b* and *il34* single, double and triple mutants. *n*=29 (siblings); 23 (*csf1a*$_{mut}$); 22 (*csf1b*$_{mut}$); 4 (*il34*$_{mut}$); 36 (*csf1a*$_{mut}$*csf1b*$_{mut}$); 8 (*csf1a*$_{mut}$*il34*$_{mut}$); 8 (*csf1b*$_{mut}$*il34*$_{mut}$); 11 (*csf1a*$_{mut}$*csf1b*$_{mut}$ *il34*$_{mut}$). (C) WISH of *cmyb* at 4 dpf in ABSR (wild type) (*n*=9) and *Tg*(*hsp70:csf1a*) fish (*n*=52). Both embryos were heat shocked at 37°C in a water bath for 1 h at 2 dpf, 2.5 dpf and 3 dpf. Red arrowheads indicate *cmyb*$^{+}$ HSPCs. (D) WISH of *cmyb* at 4 dpf in ABSR (*n*=8) and *Tg*(*hsp70:csf1b*) fish (*n*=50). Both embryos were heat shocked at 37°C in a water bath for 1 h at 2 dpf, 2.5 dpf and 3 dpf. Red arrowheads indicate *cmyb*$^{+}$ HSPCs. (E) WISH of *cmyb* at 3.5 dpf in ABSR (*n*=15) and *Tg*(*hsp70:il34*) fish (*n*=27). Both embryos were heat shocked at 37°C in a water bath for 1 h at 2 dpf, 2.5 dpf and 3 dpf. Red arrowheads indicate *cmyb*$^{+}$ HSPCs. Data are presented as mean±s.e.m. ns, not significant.

myelocytes and lymphocytes (Figs 2 and 3, Fig. S3). In the adult fish kidney, hematopoietic defects remained severe, but erythroid cells recovered (Fig. 4, Fig. S12A-C).

Csf1r is regarded as a major regulator of myeloid cell development in vertebrates. Here, our data reveal the function of Csf1rb in the higher hierarchy during hematopoiesis. Some reports have suggested that CSF1R may function in HSCs or progenitors in mammals. For instance, CSF1R has been detected in HSPCs (Miyamoto et al., 2002). In *Csf1*$^{op/op}$ or *Csf1r* mutant mice or rats, both blood lymphocytes and monocytes were decreased (Dai et al., 2002; Keshvari et al., 2021; Pridans et al., 2018). However, no detailed analysis of the populating ability of HSPCs, such as a transplantation assay with HSPCs from CSF1R signaling-deficient mice, has been performed, and most of the data is based on the colony formation assay that may not be able to reveal the function of CSF1R in HSPCs. Recently, it has been reported that PLX5622, a chemical inhibitor presumably targeting CSF1R, can reduce HSC and hematopoietic progenitors in adult mouse bone marrow (Lei et al., 2020). On the contrary, abolishing *Csf1r* expression in the bone marrow via deletion of a *csf1r* enhancer shows no effects on hematopoietic progenitors (Rojo et al., 2019). Therefore, whether CSF1R in mouse or human is similar to Csf1rb in zebrafish in regulating HSPC maintenance remains unclear and needs further exploration.

The expression of *csf1rb* in HSPCs (Fig. 1) and HSPC defects in *csf1rb* mutants (Fig. 2F-I, Fig. S3A-C) strongly suggest that T-cell defects in *csf1rb* mutants are related to the cell-autonomous effect of *csf1rb* in HSPCs. Yu et al. reported that in *pu.1/spi1b* double-deficiency zebrafish larvae, macrophages were severely disrupted before 8 dpf, but the *rag1*$^{+}$ T cells at 5 dpf were not affected (Yu et al., 2017). Faiza et al. showed that *csf3r* mutation caused a significant reduction of neutrophils, but the *rag1*$^{+}$ T cells at 5 dpf were normal (Basheer et al., 2019). These studies suggest that myeloid cell defects have little impact on T-cell development in early zebrafish larvae. Therefore, the T-cell defects in the *csf1rb* mutant were unlikely an indirect consequence of the myeloid cell defects.

The BrdU assay is a well-established method to detect cell proliferation. BrdU incorporation occurs when the synthesis of DNA is ongoing. Usually, a short duration of BrdU application

Development (2022) 149, dev200534. doi:10.1242/dev.200534

labels S-phase cells, whereas a longer duration labels both proliferating and proliferated cells. We performed BrdU labeling over a short time (within 1 h), which is not long enough for normal cells to complete a whole cell cycle. Therefore, the 0.5 ratio may not mean that half of all *cmyb*:GFP$^+$ cells proliferated within 1 h of BrdU labeling. Instead, it suggests that about half of all *cmyb*:GFP$^+$ cells were undergoing DNA synthesis within this short incubation time. This HSPC proliferation rate was similar to the BrdU$^+$ incorporation ratio of HSPCs reported in other studies at around 2-3 dpf, when the BrdU incorporation was performed within 1-3 h (Xia et al., 2021; Xue et al., 2017; Zhang et al., 2011).

A recent publication by Ferrero et al. about zebrafish *csf1rb* mutants concluded that *csf1rb* deficiency predominantly affected myeloid and B-lineage development (Ferrero et al., 2020). These results are within the scope of the previous understanding of Csf1r functions in downstream hematopoietic lineages such as myeloid cells. In contrast, our findings clearly showed that HSPCs were impaired in *csf1rb* mutants. This conclusion is supported by three different experiments: the decrease of definitive hematopoietic cells in embryonic/adult *csf1rb* mutants, the impaired definitive hematopoiesis in a complementary test with two different *csf1rb* mutant alleles, and the failure of hematopoietic reconstitution after transplantation with the kidney marrow cells from *csf1rb* mutants. The difference between Ferrero's and our findings may be attributed to the use of different *csf1rb* mutant alleles. Ferrero's *csf1rb* mutant allele led to a splicing defect and an additional isoform of *csf1rb* was observed in Ferrero's study. Therefore, Ferrero's *csf1rb* mutant allele may not fully abolish *csf1rb* functions. In contrast, four exons were deleted in our *csf1rb* mutant allele to ensure the full loss of *csf1rb* functions.

Surprisingly, the phenotype for erythroid lineages in *csf1rb* mutant fish was not consistent between embryonic stages and adulthood, as the defects of mature erythroid cells in *csf1rb* mutant fish recovered in the early juvenile to adult stage (Fig. 4C,D, Fig. S12). This phenotype is in accordance with normal red blood cells in *Csf1r* mutant rats aged between 6 and 12 weeks (Dai et al., 2002; Pridans et al., 2018), but the erythroid lineage phenotype in embryonic mutant mice or rats was not reported in the previous study. We examined the expression of *csf1rb* in the Atlas for Zebrafish Development database from the UCSC cell browser (https://cells.ucsc.edu), which contains the single-cell RNA sequencing data of 1, 2 and 5 dpf zebrafish embryos. It turned out that *csf1rb* was also detected in mature myeloid cell and lymphoid cell clusters, but not in mature erythroid cells (Fig. S14; Speir et al., 2021). In addition, we have shown that *csf1rb* depletion did not interfere with the development of primitive erythroid cells, indicating that Csf1rb may not be required for the maturation of erythroid cells from *gata1*$^+$ committed precursors, but is required for the downstream development of myeloid and lymphoid cells. Some studies have suggested that under certain conditions, such as bone marrow failure, tissue inflammation, abnormal systemic chemokine production, and especially severe hematologic disorders, compensatory reactivation occurs to fulfill the need for blood cell production by increasing the maturation of downstream lineages (Johns and Christopher, 2012). Thus, we speculate that the deficiency of erythroid lineages at early stages may lead to hypoxia. As the maturation of myeloid and lymphoid cells depends on Csf1rb, but erythroid cell maturation does not rely on Csf1rb, the compensatory hematopoiesis compromises erythroid but not myeloid and lymphoid defects over time.

Zebrafish orthologs of dedicated ligands for CSF1R in mammals, including Csf1a/Csf1b and Il34, have been demonstrated to work through Csf1ra to regulate xanthophore cell development or microglial colonization in the brain, respectively (Kuil et al., 2019; Parichy and Turner, 2003; Patterson et al., 2014; Wu et al., 2018). Surprisingly, none of these ligands is likely to be the ligand for Csf1rb in regulating HSPCs, as suggested by the loss-of-function and gain-of-function studies (Fig. 6). Cytokines, such as IL3, IL5, CSF2, and the ligand of Flt3 are involved in hematopoiesis in mammals. However, they have not been identified in zebrafish (Bartunek et al., 2018). Interestingly, the whole gene cluster for *IL3*, *IL5* and *CSF2* is depleted in the zebrafish genome, and the receptor genes were also not identified. The function of these genes may be compensated for by other regulators (Liongue and Ward, 2007). Recently, the Flt3 receptor was identified in zebrafish and was shown to be important for the development of definitive HSPCs (He et al., 2014). However, the Flt3 ligand in zebrafish is still unknown. The poor sequence homology of cytokines between zebrafish and mammals has made it challenging to identify new cytokine orthologs in zebrafish. Therefore, the ligand for Csf1rb may be an unknown gene. Alternatively, other known cytokines may work through Csf1rb to regulate HSPCs in zebrafish. Different cytokines may have the ability to activate the same receptor to exert similar functions (Ozaki and Leonard, 2002). For instance, CXCL9, CXCL10 and CXCL11 share the receptor CXCR3 and mediate overlapping effects in T cells and intestinal myofibroblasts (Campanella et al., 2008; Kouroumalis et al., 2005). CSF2, IL3 and IL5 regulate the differentiation and function of eosinophils via a common β receptor subunit during airway inflammation (Asquith et al., 2008). The redundancy of cytokines reminds us that multiple cytokines may function through Csf1rb to regulate HSPC maintenance, and they are not limited to Csf1/Il34, which may explain why both gain of function and loss of function in Csf1/Il34 resulted in no obvious HSPC phenotype. Other cytokines that have been reported in the hematopoietic system may participate in the regulation of HSPCs via Csf1rb. Further study is required to address the ligand for Csf1rb in zebrafish.

MATERIALS AND METHODS

Zebrafish

All zebrafish lines were raised and maintained according to standard protocols (Westerfield, 2000). In this study, ABSR wild type, *Tg(flk1:mCherry)* and *Tg(flk1:GFP)* (Choi et al., 2007), *Tg(cmyb:GFP)* (North et al., 2007), *Tg(runx1:en-GFP)* (Zhang et al., 2015), *Tg(mpeg1:GFP)*, *Tg(flk1:NLS-Eos)* (Fukuhara et al., 2014), *Tg(coro1a:DsRedx)* (Xu et al., 2016), *Tg(coro1a:Kaede)* (Zhan et al., 2018), *Tg(globin:GFP)*, *Tg (globin:loxP-DsRedx-loxP-GFP)*, *Tg (lck:loxP-DsRedx-loxP-GFP)* (Tian et al., 2017), *Tg(hsp70:csf1a)*, *Tg(hsp70:csf1b)*, *Tg(hsp70:il34)*, *Runx1*^{w84x} (Jin et al., 2009), *csf1ra*^{j4e1}(Herbomel et al., 2001), *csf1rb*^{re01} (Oosterhof et al., 2018), *csf1a*^{hkz9}, *csf1b*^{hkz10}, *il34*^{hkz11} (Wu et al., 2018) and *csf1rb*^{hkz15} were used.

All animal experiments were performed under the approval of the Animal Ethics Committees of the Hong Kong University of Science and Technology and South China University of Technology.

Mutant and transgenic line generation

The *csf1rb* mutant fish line was generated by the CRISPR-Cas9 method following previous reports (Chang et al., 2013; Wu et al., 2018). The *csf1rb* mutant was identified with primers 5′-GTTCACCATACCAATGTGGC-3′ and 5′-AGCATTCACAGACTGGCTGA-3′ for the mutant allele, 5′-ATTG-ACCCCAGCCAACTTCC-3′ and 5′-TAGCGTAGCCTAGAGGCCTA-3′ for the wild-type allele.

To generate *Tg(hsp70:csf1a)*, *Tg(hsp70:csf1b)* and *Tg(hsp70:il34)*, the promoter of zebrafish heat shock protein 70 (*hsp70*) was constructed into the pBSK vector with minimal Tol2 transposon sequence and an SV40 polyA sequence, and the cDNA of *csf1a, csf1b* or *il34* was cloned under the control of the promoter. Plasmid injection and stable line screening were performed as previously described (Wu et al., 2018).

Development (2022) 149, dev200534. doi:10.1242/dev.200534

WISH

WISH of *csf1ra*, *csf1rb*, *cmyb*, *runx1*, *pu.1*, *mfap4*, *lck*, *rag1*, *gata1*, *αe1-globin* and *βe2-globin* was performed as previously described (Wu et al., 2018).

Immunofluorescence staining and imaging

Immunofluorescent antibody staining was conducted following previous studies (Dai et al., 2016). The primary antibodies utilized in this study were: rabbit anti-DsRedx antibody (632496; Clontech; 1:400), goat anti-GFP antibody (ab6658; Abcam; 1:400), rabbit anti-Gata1 (ab210539, Abcam; 1:100), mouse anti-BrdU (1117037600, Roche; 1:50), rabbit anti-Lcp1 (Jin et al., 2009; 1:400) and rabbit anti-AE1-globin (Du et al., 2011; 1:400). Secondary antibodies used in this study were: Alexa 488 anti-goat antibody (A11055, Invitrogen), Alexa 555 anti-rabbit antibody (A31572, Invitrogen), Alexa 488 anti-rabbit antibody (A21206, Invitrogen), Alexa 555 anti-mouse antibody (A31570, Invitrogen). All of the images were taken with Leica SP8 or Zeiss LSM800 confocal microscope and the quantification was conducted manually.

BrdU labeling and immunostaining

The BrdU-based proliferation assay was performed as previously reported (Dai et al., 2016). In brief, embryos were incubated with BrdU for 30 min followed by 30 min recovery before fixation. Before 2 N HCl treatment, the head region was cut for genome typing. Embryos were separated according to genome types and stained with anti-BrdU and anti-GFP antibodies simultaneously.

TUNEL assay and histological staining

A cell death assay based on TUNEL was performed as previously described (Dai et al., 2016). Neutral Red staining was conducted as previously described (Dai et al., 2016).

Photo-conversion and time-lapse confocal microscopic imaging

Photo-conversion was conducted with a 405-nm UV laser as previously described (Tian et al., 2017). For the HSPC budding assay, nine endothelia in the VDA for each fish were converted with one per somite at 28-30 hpf. Live imaging was performed immediately for about 26 h with a time interval of 10.8 min. For cell conversion in the *Tg(coro1a: Kaede)* line, kaede^{+} cells from the VDA region were converted at 2.5 or 3 dpf, respectively. Live imaging of the VDA region was conducted right after conversion for overnight. Live imaging of HSPCs in the *Tg(cmyb:GFP)* line was captured from 2.5 dpf for about 26 h with a time interval of 4 or 6 min. All time-lapse imaging was captured using a Leica SP8 confocal microscope.

Heat shock procedure

Heat shock was performed in a 37°C water bath for 1 h at 2, 2.5 and 3 dpf.

Flow cytometry and WKM transplantation

Flow cytometry was performed with BD FACS Aria III, and data were analyzed on BD FACS Aria III or FlowJo. Adult fish kidney marrow cell suspension was prepared according to a previous study (Tian et al., 2017). The concentration of adult whole kidney marrow cell suspension was determined using a hemocytometer, and 2.4×10^5 cells were prepared in 2 µl injection medium containing 1.8 U heparin (Sigma-Aldrich) and 0.4 U DNaseI (QIAGEN) in 5% fetal bovine serum (FBS) in PBS; 3.5 nl of the cell solution was injected into the circulation of 2 dpf *runx1* mutant embryos injected with *pu.1* morpholino (Gene Tools).

For 11 dpf juvenile fish, fish were anesthetized and killed on ice, then two fish were grouped in 5% FBS in PBS and homogenized with a 24 or 27 gauge needle. The cell suspension was filtered through a 40-µm nylon mesh before flow cytometry analysis (FACS Aria III; BD Biosciences). In addition, 40 µl adult peripheral blood was collected from each fish into 500 µl 5% FBS/PBS for FACS analysis and 10 µl peripheral blood was collected in 100 µl 3 U/µl heparin in 5% FBS/PBS to perform May–Grunwald and Giemsa staining as previously described (Lin et al., 2019).

Thymus area quantification

Tg(coro1a:DsRedx) fish at 45 dpf were anesthetized and body length measured. The skin and bone covering the thymus were removed and imaged under a Zeiss LSM800 confocal microscope. The thymus area indicated by *rag1*/*lck* expression at 5 dpf or by *coro1a*-DsRedx expression at 45 dpf was manually marked according to the signal and defined automatically using ZEISS ZEN microscope software.

Quantification of surface brightness intensity

After heat-shock treatment, wild-type control fish and *Tg(hsp70:csf1a)* or *Tg(hsp70:csf1b)* fish were collected and anesthetized, and imaged using a Zeiss AXIO Zoom.V16 microscope. The surface region of each individual fish was marked with same size and location, and the mean intensity value of the bright channel within the marked region was determined automatically using ZEISS ZEN microscope software.

Quantitative real-time PCR (Q-PCR)

The relative expression level of *csf1rb* in *csf1rb* siblings and mutants were determined by QPCR. In brief, 4 dpf individual embryos were subjected to lysis, and, after genotyping, sibling and mutant embryos were pooled together for total RNA extraction with the RNeasy mini kit (QIAGEN, 74104), and cDNA was obtained using the SuperScript II reverse transcription kit (Thermo Fisher Scientific, 18064022). The expression of *csf1rb* was normalized to *ef1a* (*eef1a1l1*). The primers for *csf1rb* were 5′-GATGCTCTGTGTCGCTCTCAT-3′ and 5′-TCTGCGCCTGGTCTTC-CATA-3′; primers for *ef1a* were 5′-CTTCTCAGGCTGACTGTGC-3′ and 5′-CCGCTAGCATTACCCTCC-3′.

Quantification and statistical analysis

All the statistical analysis was performed using GraphPad Prism version 8 with unpaired Student's *t*-tests, and two-tailed *P*-values were used for all *t*-tests.

Acknowledgements

We would like to thank Prof. Tjakko J. van Ham from the University Medical Center for sharing the *csf1rb*^{re01} zebrafish mutant line, and Prof. Feng Liu from Chinese Academy of Science for sharing the *Tg(runx1:en-GFP)* fish. We thank International Science Editing (https://www.internationalscienceediting.com/) for editing this manuscript.

Competing interests

The authors declare no competing or financial interests.

Author contributions

Conceptualization: Y.D., S.W.; Methodology: Y.D.; Validation: Y.D.; Formal analysis: Y.D., S.W., C.C., R.X., X.L.; Investigation: Y.D.; Data curation: Y.D.; Writing - original draft: Y.D.; Writing - review & editing: S.W., Z.W., J.X.; Visualization: Y.D.; Supervision: Z.W., J.X.; Project administration: Z.W., J.X.; Funding acquisition: Z.W., J.X.

Funding

This work was supported by the National Key Research and Development Program of China (2018YFA0800200), National Natural Science Foundation of China (31771594, 31970763), Science and Technology Planning Project of Guangdong Province (2019A030317001), National Natural Science Foundation of China/Research Grants Council, University Grants Committee Joint Research Scheme (31961160726), Research Grants Council, University Grants Committee (16103718; N_HKUST621/17; C6002-17GF), Innovation and Technology Commission of the HKSAR (ITCPD/17-9) and Science and Technology Projects in Guangzhou (202201010116).

Peer review history

The peer review history is available online at https://journals.biologists.com/dev/article-lookup/doi/10.1242/dev.200534.reviewer-comments.pdf.

References

Amsellem, S., Pflumio, F., Bardinet, D., Izac, B., Charneau, P., Romeo, P.-H., Dubart-Kupperschmitt, A. and Fichelson, S. (2003). Ex vivo expansion of human hematopoietic stem cells by direct delivery of the HOXB4 homeoprotein. *Nat. Med.* **9**, 1423-1427. doi:10.1038/nm953

Arai, F., Hirao, A., Ohmura, M., Sato, H., Matsuoka, S., Takubo, K., Ito, K., Koh, G. Y. and Suda, T. (2004). Tie2/Angiopoietin-1 signaling regulates hematopoietic stem cell quiescence in the bone marrow niche. *Cell* **118**, 149-161. doi:10.1016/j.cell.2004.07.004

Asquith, K. L., Ramshaw, H. S., Hansbro, P. M., Beagley, K. W., Lopez, A. F. and Foster, P. S. (2008). The IL-3/IL-5/GM-CSF common receptor plays a pivotal role in the regulation of Th2 immunity and allergic airway inflammation. *J. Immunol.* **180**, 1199-1206. doi:10.4049/jimmunol.180.2.1199

Bartunek, P., Oltova, J. and Svobada, O. (2018). Hematopoietic cytokine gene duplication in zebrafish erythroid and myeloid lineages. *Front. Cell Dev. Biol.* **6**, 1-8. doi:10.3389/fcell.2018.00174

Basheer, F., Rasighaemi, P., Liongue, C. and Ward, A. C. (2019). Zebrafish granulocyte colony-stimulating factor receptor maintains neutrophil number and function throughout the life span. *Infect. Immun.* **87**, e00793-18. doi:10.1128/IAI.00793-18

Bertrand, J. Y., Kim, A. D., Teng, S. and Traver, D. (2008). CD41+ cmyb+ precursors colonize the zebrafish pronephros by a novel migration route to initiate adult hematopoiesis. *Development* **135**, 1853-1862. doi:10.1242/dev.015297

Böiers, C., Carrelha, J., Lutteropp, M., Luc, S., Green, J. C. A., Azzoni, E., Woll, P. S., Mead, A. J., Hultquist, A., Swiers, G. et al. (2013). Lymphomyeloid contribution of an immune-restricted progenitor emerging prior to definitive hematopoietic stem cells. *Stem Cell* **13**, 535-548. doi:10.1016/j.stem.2013.08.012

Boisset, J.-C., van Cappellen, W., Andrieu-Soler, C., Galjart, N., Dzierzak, E. and Robin, C. (2010). In vivo imaging of haematopoietic cells emerging from the mouse aortic endothelium. *Nature* **464**, 116-120. doi:10.1038/nature08764

Bowie, M. B., McKnight, K. D., Kent, D. G., McCaffrey, L., Hoodless, P. A. and Eaves, C. J. (2006). Hematopoietic stem cells proliferate until after birth and show a reversible phase-specific engraftment defect. *J. Clin. Invest.* **116**, 2808-2816. doi:10.1172/JCI28310

Braasch, I., Salzburger, W. and Meyer, A. (2006). Asymmetric evolution in two fish-specifically duplicated receptor tyrosine kinase paralogons involved in teleost coloration. *Mol. Biol. Evol.* **23**, 1192-1202. doi:10.1093/molbev/msk003

Broxmeyer, H. E., Orschell, C. M., Clapp, D. W., Hangoc, G., Cooper, S., Plett, P. A., Liles, W. C., Li, X., Graham-Evans, B., Campbell, T. B. et al. (2005). Rapid mobilization of murine and human hematopoietic stem and progenitor cells with AMD3100, a CXCR4 antagonist. *J. Exp. Med.* **201**, 1307-1318. doi:10.1084/jem.20041385

Caetano-Lopes, J., Henke, K., Urso, K., Duryea, J., Charles, J. F., Warman, M. L. and Harris, M. P. (2020). Unique and non-redundant function of csf1r paralogues in regulation and evolution of post-embryonic development of the zebrafish. *Development* **147**, dev181834. doi:10.1242/dev.181834

Campanella, G. S. V., Medoff, B. D., Manice, L. A., Colvin, R. A. and Luster, A. D. (2008). Development of a novel chemokine-mediated in vivo T cell recruitment assay. *J. Immunol. Methods* **331**, 127-139. doi:10.1016/j.jim.2007.12.002

Chang, N., Sun, C., Gao, L., Zhu, D., Xu, X., Zhu, X., Xiong, J.-W. and Xi, J. J. (2013). Genome editing with RNA-guided Cas9 nuclease in Zebrafish embryos. *Cell Res.* **23**, 465-472. doi:10.1038/cr.2013.45

Choi, J., Dong, L., Ahn, J., Dao, D., Hammerschmidt, M. and Chen, J.-N. (2007). FoxH1 negatively modulates flk1 gene expression and vascular formation in zebrafish. *Dev. Biol.* **304**, 735-744. doi:10.1016/j.ydbio.2007.01.023

Cumano, A., Ferraz, J. C., le Klaine, M., Di Santo, J. P. and Godin, I. (2001). Intraembryonic, but Not Yolk Sac hematopoietic precursors, isolated before circulation, provide long-term multilineage reconstitution. *Immunity* **15**, 477-485. doi:10.1016/S1074-7613(01)00190-X

Dai, X.-M., Ryan, G. R., Hapel, A. J., Dominguez, M. G., Russell, R. G., Kapp, S., Sylvestre, V. and Stanley, E. R. (2002). Targeted disruption of the mouse colony-stimulating factor 1 receptor gene results in osteopetrosis, mononuclear phagocyte deficiency, increased primitive progenitor cell frequencies, and reproductive defects. *Blood* **99**, 111-120. doi:10.1182/blood.V99.1.111

Dai, Y., Zhu, L., Huang, Z., Zhou, M., Jin, W., Liu, W., Xu, M., Yu, T., Zhang, Y., Wen, Z. et al. (2016). Cebpa is essential for the embryonic myeloid progenitor and neutrophil maintenance in zebrafish. *J. Genet. Genomics* **43**, 593-600. doi:10.1016/j.jgg.2016.09.001

Davidson, A. J. and Zon, L. I. (2004). The 'definitive' (and 'primitive') guide to zebrafish hematopoiesis. *Oncogene* **23**, 7233-7246. doi:10.1038/sj.onc.1207943

Deshpande, S., Bosbach, B., Yozgat, Y., Park, C. Y., Moore, M. A. S. and Besmer, P. (2013). KIT receptor gain-of-function in hematopoiesis enhances stem cell self-renewal and promotes progenitor cell expansion. *Stem Cells* **31**, 1683-1695. doi:10.1002/stem.1419

Du, L., Xu, J., Li, X., Ma, N., Liu, Y., Peng, J., Osato, M., Zhang, W. and Wen, Z. (2011). Rumba and Haus3 are essential factors for the maintenance of hematopoietic stem/progenitor cells during zebrafish hematopoiesis. *Development* **138**, 619-629. doi:10.1242/dev.054536

Ellett, F., Pase, L., Hayman, J. W., Andrianopoulos, A. and Lieschke, G. J. (2011). *mpeg1* promoter transgenes direct macrophage-lineage expression in zebrafish. *Blood* **117**, e49-e56. doi:/10.1182/blood-2010-10-314120

Ferrero, G., Miserocchi, M., Di Ruggiero, E. and Wittamer, V. (2020). A csf1rb mutation uncouples two waves of microglia development in zebrafish. *Development* **148**, dev194241. doi:10.1242/dev.194241

Fraint, E., Norberto, M. F. and Bowman, T. V. (2020). A novel conditioning-free hematopoietic stem cell transplantation model in zebrafish. *Blood Adv.* **4**, 6189-6198. doi:10.1182/bloodadvances.2020002424

Fukuhara, S., Zhang, J., Yuge, S., Ando, K., Wakayama, Y., Sakaue-Sawano, A., Miyawaki, A. and Mochizuki, N. (2014). Visualizing the cell-cycle progression of endothelial cells in zebrafish. *Dev. Biol.* **393**, 10-23. doi:10.1016/j.ydbio.2014.06.015

Ganis, J. J., Hsia, N., Trompouki, E., de Jong, J. L. O., DiBiase, A., Lambert, J. S., Jia, Z., Sabo, P. J., Weaver, M., Sandstrom, R. et al. (2012). Zebrafish globin switching occurs in two developmental stages and is controlled by the LCR. *Dev. Biol.* **366**, 185-194. doi:10.1016/j.ydbio.2012.03.021

Gering, M. and Patient, R. (2005). Hedgehog signaling is required for adult blood stem cell formation in zebrafish embryos. *Dev. Cell* **8**, 389-400. doi:10.1016/j.devcel.2005.01.010

Grabert, K., Sehgal, A., Irvine, K. M., Wollscheid-Lengeling, E., Ozdemir, D. D., Stables, J., Luke, G. A., Ryan, M. D., Adamson, A., Humphreys, N. E., et al. (2020). A transgenic line that reports CSF1R protein expression provides a definitive marker for the mouse mononuclear phagocyte system. *J. Immunol.* **205**, 3154-3166. doi:10.4049/jimmunol.2000835

Hason, M., Mikulasova, T., Machonova, O., Pombinho, A. R., Ham, T. J., van Irion, U., Nüsslein-Volhard, C., Bartunek, P. and Svoboda, O. (2022). M-CSFR/CSF1R signaling regulates myeloid fates in zebrafish via distinct action of its receptors and ligands. *Blood Adv.* **6**, 1474-1488. doi:10.1101/2021.04.06.438628

Hatzimichael, E. and Tuthill, M. (2010). Hematopoietic stem cell transplantation. *Stem Cell Cloning Adv. Appl.* **3**, 105-117. doi:10.2147/SCCAA.S6815

He, B.-L., Shi, X., Man, C. H., Ma, A. C. H., Ekker, S. C., Chow, H. C. H., So, C. W. E., Choi, W. W. L., Zhang, W., Zhang, Y. et al. (2014). Function of flt3 in zebrafish hematopoiesis and its relevance to human acute myeloid leukemia. *Blood* **123**, 2518-2529. doi:10.1182/blood-2013-02-486688

He, S., Tian, Y., Feng, S., Wu, Y., Shen, X., Chen, K., He, Y., Sun, Q., Li, X., Xu, J. et al. (2020). In vivo single-cell lineage tracing in zebrafish using high-resolution infrared laser-mediated gene induction microscopy. *eLife* **9**, e52024. doi:10.7554/eLife.52024

Heldin, C.-H. and Lennartsson, J. (2013). Structural and functional properties of platelet-derived growth factor and stem cell factor receptors. *Cold Spring Harb. Perspect. Biol.* **5**, a009100. doi:10.1101/cshperspect.a009100

Herbomel, P., Thisse, B. and Thisse, C. (2001). Zebrafish early macrophages colonize cephalic mesenchyme and developing brain, retina, and epidermis through a M-CSF receptor-dependent invasive process. *Dev. Biol.* **238**, 274-288. doi:10.1006/dbio.2001.0393

Huang, J., Nguyen-McCarty, M., Hexner, E. O., Danet-Desnoyers, G. and Klein, P. S. (2012). Maintenance of hematopoietic stem cells through regulation of Wnt and mTOR pathways. *Nat. Med.* **18**, 1778-1785. doi:10.1038/nm.2984

Huang, Y., Lu, Y., He, Y., Feng, Z., Zhan, Y., Huang, X., Liu, Q., Zhang, J., Li, H., Huang, H. et al. (2019). Ikzf1 regulates embryonic T lymphopoiesis via Ccr9 and Irf4 in zebrafish. *J. Biol. Chem.* **294**, 16152-16163. doi:10.1074/jbc.RA119.009883

Jagannathan-Bogdan, M. and Zon, L. I. (2013). Hematopoiesis. *Development* **140**, 2463-2467. doi:10.1242/dev.083147

Jin, H., Xu, J. and Wen, Z. (2007). Migratory path of definitive hematopoietic stem/progenitor cells during zebrafish development. *Blood* **109**, 5208-5214. doi:10.1182/blood-2007-01-069005

Jin, H., Sood, R., Xu, J., Zhen, F., English, M. A., Liu, P. P. and Wen, Z. (2009). Definitive hematopoietic stem/progenitor cells manifest distinct differentiation output in the zebrafish VDA and PBI. *Development* **136**, 1397. doi:10.1242/dev.036780

Johns, J. L. and Christopher, M. M. (2012). Extramedullary hematopoiesis: a new look at the underlying stem cell niche, theories of development, and occurrence in animals. *Vet. Pathol.* **49**, 508-523. doi:10.1177/0300985811432344

Keshvari, S., Caruso, M., Teakle, N., Batoon, L., Sehgal, A., Patkar, O. L., Ferrari-Cestari, M., Snell, C. E., Chen, C., Stevenson, A. et al. (2021). CSF1R-dependent macrophages control postnatal somatic growth and organ maturation. *PLoS Genet.* **17**, e1009605. doi:10.1371/journal.pgen.1009605

Kieusseian, A., Brunet de la Grange, P., Burlen-Defranoux, O., Godin, I. and Cumano, A. (2012). Immature hematopoietic stem cells undergo maturation in the fetal liver. *Development* **139**, 3521-3530. doi:10.1242/dev.079210

Kimura, S., Roberts, A. W., Metcalf, D. and Alexander, W. S. (1998). Hematopoietic stem cell deficiencies in mice lacking c-Mpl, the receptor for thrombopoietin. *Proc. Natl. Acad. Sci. USA* **95**, 1195-1200. doi:10.1073/pnas.95.3.1195

Kissa, K. and Herbomel, P. (2010). Blood stem cells emerge from aortic endothelium by a novel type of cell transition. *Nature* **464**, 112-115. doi:10.1038/nature08761

Kouroumalis, A., Nibbs, R. J., Aptel, H., Wright, K. L., Kolios, G. and Ward, S. G. (2005). The chemokines CXCL9, CXCL10, and CXCL11 differentially stimulate

G alpha i-independent signaling and actin responses in human intestinal myofibroblasts. *J. Immunol.* **175**, 5403-5411. doi:10.4049/jimmunol.175.8.5403

Kuil, L. E., Oosterhof, N., Geurts, S. N., van der Linde, H. C., Meijering, E. and van Ham, T. J. (2019). Reverse genetic screen reveals that Il34 facilitates yolk sac macrophage distribution and seeding of the brain. *Dis. Model. Mech.* **12**, dmm037762. doi:10.1242/dmm.037762

Kumar, J. and Geiger, H. (2017). HSC Niche biology and HSC expansion ex vivo. *Trends Mol. Med.* **23**, 799-819. doi:10.1016/j.molmed.2017.07.003

Lam, E. Y. N., Hall, C. J., Crosier, P. S., Crosier, K. E. and Flores, M. V. (2010). Live imaging of Runx1 expression in the dorsal aorta tracks the emergence of blood progenitors from endothelial cells. *Blood* **116**, 909-914. doi:10.1182/blood-2010-01-264382

Langenau, D. M., Ferrando, A. A., Traver, D., Kutok, J. L., Hezel, J.-P. D., Kanki, J. P., Zon, L. I., Look, A. T. and Trede, N. S. (2004). In vivo tracking of T cell development, ablation, and engraftment in transgenic zebrafish. *Proc. Natl. Acad. Sci. U.S.A.* **101**, 7369-7374. doi:10.1073/pnas.0402248101

Lei, F., Cui, N., Zhou, C., Chodosh, J., Vavvas, D. G. and Paschalis, E. I. (2020). CSF1R inhibition by a small-molecule inhibitor is not microglia specific; affecting hematopoiesis and the function of macrophages. *Proc. Natl. Acad. Sci. USA* **117**, 23336-23338. doi:10.1073/pnas.1922788117

Li, L., Yan, B., Shi, Y.-Q., Zhang, W.-Q. and Wen, Z.-L. (2012). Live imaging reveals differing roles of macrophages and neutrophils during zebrafish tail fin regeneration. *J. Biol. Chem.* **287**, 25353-25360. doi:10.1074/jbc.M112.349126

Lin, X., Zhou, Q., Zhao, C., Lin, G., Xu, J. and Wen, Z. (2019). An ectoderm-derived myeloid-like cell population functions as antigen transporters for Langerhans cells in zebrafish epidermis. *Dev. Cell* **49**, 605-617.e5. doi:10.1016/j.devcel.2019.03.02

Liongue, C. and Ward, A. C. (2007). Evolution of Class I cytokine receptors. *BMC Evol. Biol.* **7**, 120. doi:10.1186/1471-2148-7-120

Lis, R., Karrasch, C. C., Poulos, M. G., Kunar, B., Redmond, D., Duran, J. G. B., Badwe, C. R., Schachterle, W., Ginsberg, M., Xiang, J. et al. (2017). Conversion of adult endothelium to immunocompetent haematopoietic stem cells. *Nature* **545**, 439-445. doi:10.1038/nature22326

Matsunaga, T., Kato, T., Miyazaki, H. and Ogawa, M. (1998). Thrombopoietin promotes the survival of murine hematopoietic long-term reconstituting cells-comparison with the effects of FLT3:FLK-2 ligand and Interleukin-6. *Blood* **92**, 452-461. doi:10.1182/blood.V92.2.452

Meijer, A. H., van der Sar, A. M., Cunha, C., Lamers, G. E. M., Laplante, M. A., Kikuta, H., Bitter, W., Becker, T. S. and Spaink, H. P. (2008). Identification and real-time imaging of a myc-expressing neutrophil population involved in inflammation and mycobacterial granuloma formation in zebrafish. *Dev. Comp. Immunol.* **32**, 36-49. doi:10.1016/j.dci.2007.04.003

Millard, S. M., Heng, O., Opperman, K. S., Sehgal, A., Irvine, K. M., Kaur, S., Sandrock, C. J., Wu, A. C., Magor, G. W., Batoon, L. et al. (2021). Fragmentation of tissue-resident macrophages during isolation confounds analysis of single-cell preparations from mouse hematopoietic tissues. *Cell Rep.* **37**, 110058. doi:10.1016/j.celrep.2021.110058

Miyamoto, T., Iwasaki, H., Reizis, B., Ye, M., Graf, T., Weissman, I. L. and Akashi, K. (2002). Myeloid or lymphoid promiscuity as a critical step in hematopoietic lineage commitment. *Dev. Cell* **3**, 137-147. doi:10.1016/S1534-5807(02)00201-0

Mizuno, H., Mal, T. K., Tong, K. I., Ando, R., Furuta, T., Ikura, M. and Miyawaki, A. (2003). Photo-induced peptide cleavage short article in the green-to-red conversionof a fluorescent protein. *Mol. Cell* 12, 1051-1058. doi:10.1016/S1097-2765(03)00393-9

Monteiro, R., Pouget, C. and Patient, R. (2011). The gata1/pu.1 lineage fate paradigm varies between blood populations and is modulated by tif1γ. *EMBO J.* **30**, 1093-1103. doi:10.1038/emboj.2011.34

Mossadegh-Keller, N., Sarrazin, S., Kandalla, P. K., Espinosa, L., Stanley, E. R., Nutt, S. L., Moore, J. and Sieweke, M. H. (2016). M-CSF instructs myeloid lineage fate in single haematopoietic stem cells. *Nature* **497**, 239-243. doi:10.1038/nature12026

Murayama, E., Kissa, K., Zapata, A., Mordelet, E., Briolat, V., Lin, H.-F., Handin, R. I. and Herbomel, P. (2006). Tracing hematopoietic precursor migration to successive hematopoietic organs during zebrafish development. *Immunity* **25**, 963-975. doi:10.1016/j.immuni.2006.10.015

North, T. E., Goessling, W., Walkley, C. R., Lengerke, C., Kopani, K. R., Lord, A. M., Weber, G. J., Bowman, T. V., Jang, I.-H., Grosser, T. et al. (2007). Prostaglandin E2 regulates vertebrate haematopoietic stem cell homeostasis. *Nature* **447**, 1007-1011. doi:10.1038/nature05883

Oosterhof, N., Kuil, L. E., van der Linde, H. C., Burm, S. M., Berdowski, W., van Ijcken, W. F. J., van Swieten, J. C., Hol, E. M., Verheijen, M. H. G. and van Ham, T. J. (2018). Colony-Stimulating Factor 1 Receptor (CSF1R) regulates microglia density and distribution, but not microglia differentiation *in vivo*. *Cell Rep.* **24**, 1203-1217.e6. doi:10.1016/j.celrep.2018.06.113

Oosterhof, N., Chang, I. J., Karimiani, E. G., Kuil, L. E., Jensen, D. M., Daza, R., Young, E., Astle, L., van der Linde, H. C., Shivaram, G. M. et al. (2019). Homozygous mutations in CSF1R cause a pediatric-onset leukoencephalopathy and can result in congenital absence of microglia. *Am. J. Hum. Genet.* **104**, 936-947. doi:10.1016/j.ajhg.2019.03.010

Ozaki, K. and Leonard, W. J. (2002). Cytokine and cytokine receptor pleiotropy and redundancy. *J. Biol. Chem.* **277**, 29355-29358. doi:10.1074/jbc.R200003200

Parichy, D. M. and Turner, J. M. (2003). Temporal and cellular requirements for Fms signaling during zebrafish adult pigment pattern development. *Development* **130**, 817-833. doi:10.1242/dev.00307

Parichy, D. M., Ransom, D. G., Paw, B., Zon, L. I. and Johnson, S. L. (2000). An orthologue of the kit-related gene fms is required for development of neural crest-derived xanthophores and a subpopulation of adult melanocytes in the zebrafish, Danio rerio. *Development* **127**, 3031-3044. doi:10.1242/dev.127.14.3031

Patterson, L. B. and Parichy, D. M. (2013). Interactions with iridophores and the tissue environment required for patterning melanophores and xanthophores during zebrafish adult pigment stripe formation. *PLoS Genet.* **9**, e1003561. doi:10.1371/journal.pgen.1003561

Patterson, L. B., Bain, E. J. and Parichy, D. M. (2014). Pigment cell interactions and differential xanthophore recruitment underlying zebrafish stripe reiteration and Danio pattern evolution. *Nat. Comms.* **5**, 5299. doi:10.1038/ncomms6299

Perlin, J. R., Robertson, A. L. and Zon, L. I. (2017). Efforts to enhance blood stem cell engraftment: recent insights from zebrafish hematopoiesis. *J. Exp. Med.* **214**, 2817-2827. doi:10.1084/jem.20171069

Perry, J. M., He, X. C., Sugimura, R., Grindley, J. C., Haug, J. S., Ding, S. and Li, L. (2011). Cooperation between both Wnt/β-catenin and PTEN/PI3K/Akt signaling promotes primitive hematopoietic stem cell self-renewal and expansion. *Genes Dev.* **25**, 1928-1942. doi:10.1101/gad.17421911

Pridans, C., Raper, A., Davis, G. M., Alves, J., Sauter, K. A., Lefevre, L., Regan, T., Meek, S., Sutherland, L., Thomson, A. J. et al. (2018). Pleiotropic impacts of macrophage and microglial deficiency on development in rats with targeted mutation of the Csf1r locus. *J. Immunol.* **201**, 2683-2699. doi:10.4049/jimmunol.1701783

Rhodes, J., Hagen, A., Hsu, K., Deng, M., Liu, T. X., Look, A. T. and Kanki, J. P. (2005). Interplay of Pu.1 and Gata1 determines myelo-erythroid progenitor cell fate in zebrafish. *Dev. Cell* **8**, 97-108. doi:10.1016/j.devcel.2004.11.014

Rojo, R., Raper, A., Ozdemir, D. D., Lefevre, L., Grabert, K., Wollscheid-Lengeling, E., Bradford, B., Caruso, M., Gazova, I., Sánchez, A. et al. (2019). Deletion of a Csf1r enhancer selectively impacts CSF1R expression and development of tissue macrophage populations. *Nat. Comms.* **10**, 1-17. doi:10.1038/s41467-019-11053-8

Sinclair, A., Park, L., Shah, M., Drotar, M., Calaminus, S., Hopcroft, L. E. M., Kinstrie, R., Guitart, A. V., Dunn, K., Abraham, S. A. et al. (2016). CXCR2 and CXCL4 regulate survival and self-renewal of hematopoietic stem/progenitor cells. *Blood* **128**, 371-383. doi:10.1182/blood-2015-08-661785

Speir, M. L., Bhaduri, A., Markov, N. S., Moreno, P., Nowakowski, T. J., Papatheodorou, I., Pollen, A. A., Raney, B. J., Seninge, L., Kent, W. J. et al. (2021). UCSC Cell Browser: Visualize Your Single-Cell Data. *Bioinformatics* **37**, 4578-4580. doi:10.1093/bioinformatics/btab503

Stables, J., Green, E. K., Sehgal, A., Patkar, O. L., Keshvari, S., Taylor, I., Ashcroft, M. E., Grabert, K., Wollscheid-Lengeling, E., Szymkowiak, S. et al. (2022). A kinase-dead Csf1r mutation associated with adult-onset leukoencephalopathy has a dominant inhibitory impact on CSF1R signalling. *Development* **149**, dev200237. doi:10.1242/dev.200237

Stanley, E. R. and Chitu, V. (2014). CSF-1 receptor signaling in myeloid cells. *Cold Spring Harb. Perspect. Biol.* **6**, a021857. doi:10.1101/cshperspect.a021857

Tamplin, O. J., Durand, E. M., Carr, L. A., Childs, S. J., Hagedorn, E. J., Li, P., Yzaguirre, A. D., Speck, N. A. and Zon, L. I. (2015). Hematopoietic stem cell arrival triggers dynamic remodeling of the perivascular niche. *Cell* **160**, 241-252. doi:10.1016/j.cell.2014.12.032

Tan, J. C., Nocka, K., Ray, P., Traktman, P. and Besmer, P. (1990). The dominant W42 spotting phenotype results from a missense mutation in the c-kit receptor kinase. *Science* **247**, 209-212.

Tian, Y., Xu, J., Feng, S., He, S., Zhao, S., Zhu, L., Jin, W., Dai, Y., Luo, L., Qu, J. Y. et al. (2017). The first wave of T lymphopoiesis in zebrafish arises from aorta endothelium independent of hematopoietic stem cells. *J. Exp. Med.* **214**, 3347-3360. doi:10.1084/jem.20170488

Traver, D., Paw, B. H., Poss, K. D., Penberthy, W. T., Lin, S. and Zon, L. I. (2003). Transplantation and in vivo imaging of multilineage engraftment in zebrafish bloodless mutants. *Nat. Immunol.* **4**, 1238-1246. doi:10.1038/ni1007

Ulloa, B. A., Habbsa, S. S., Potts, K. S., Lewis, A., McKinstry, M., Payne, S. G., Flores, J. C., Nizhnik, A., Norberto, M. F., Mosimann, C. et al. (2021). Definitive hematopoietic stem cells minimally contribute to embryonic hematopoiesis. *Cell Rep.* **36**, 109703. doi:10.1016/j.celrep.2021.109703

Wang, Y. and Colonna, M. (2014). Interkeukin-34, a cytokine crucial for the differentiation and maintenance of tissue resident macrophages and Langerhans cells. *Eur. J. Immunol.* **44**, 1575-1581. doi:10.1002/eji.201344365

Wang, Y., Szretter, K. J., Vermi, W., Gilfillan, S., Rossini, C., Cella, M., Barrow, A. D., Diamond, M. S. and Colonna, M. (2012). IL-34 is a tissue-restricted ligand of CSF1R required for the development of Langerhans cells and microglia. *Nat. Immunol.* **13**, 753-760. doi:10.1038/ni.2360

Wei, Q. and Frenette, P. S. (2018). Niches for hematopoietic stem cells and their progeny. *Immunity* **48**, 632-648. doi:10.1016/j.immuni.2018.03.024

Westerfield, M. (2000). *The Zebrafish Book. A Guild for the Laboratory use of Zebrafish*, 4th edn. Insititute of Neuroscience, University of Oregon Press.

Wiktor-Jedrzejczak, W. W., Ahmed, A., Szczylik, C. and Skelly, R. R. (1982). Hematological characterization of congenital osteopetrosis in *op*/*op* mouse. *J. Exp. Med.* **156**, 1516-1527. doi:10.1084/jem.156.5.1516

Wohrer, S., Knapp, D. J. H. F., Copley, M. R., Benz, C., Kent, D. G., Rowe, K., Babovic, S., Mader, H., Oostendorp, R. A. J. and Eaves, C. J. (2014). Distinct stromal cell factor combinations can separately control hematopoietic stem cell survival, proliferation, and self-renewal. *Cell Rep.* **7**, 1956-1967. doi:10.1016/j.celrep.2014.05.014

Wu, S., Xue, R., Hassan, S., Nguyen, T. M. L., Wang, T., Pan, H., Xu, J., Liu, Q., Zhang, W. and Wen, Z. (2018). Il34-Csf1r pathway regulates the migration and colonization of microglial precursors. *Dev. Cell* **46**, 552-563.e4. doi:10.1016/j.devcel.2018.08.005

Xia, J., Kang, Z., Xue, Y., Ding, Y., Gao, S., Zhang, Y., Lv, P., Wang, X., Ma, D., Wang, L. et al. (2021). A single-cell resolution developmental atlas of hematopoietic stem and progenitor cell expansion in zebrafish. *Proc. Natl. Acad. Sci. USA* **118**, e2015748118. doi:10.1073/pnas.2015748118

Xu, J., Wang, T., Wu, Y., Jin, W. and Wen, Z. (2016). Microglia colonization of developing zebrafish midbrain is promoted by apoptotic neuron and lysophosphatidylcholine. *Dev. Cell* **38**, 214-222. doi:10.1016/j.devcel.2016.06.018

Xue, Y., Lv, J., Zhang, C., Wang, L., Ma, D. and Liu, F. (2017). The vascular niche regulates hematopoietic stem and progenitor cell lodgment and expansion via klf6a-ccl25b. *Dev. Cell* **42**, 349-362.e4. doi:10.1016/j.devcel.2017.07.012

Xue, R., Wang, Y., Wang, T., Lyu, M., Mo, G., Fan, X., Li, J., Yen, K., Yu, S., Liu, Q. et al. (2021). Functional verification of novel ELMO1 variants by live imaging in zebrafish. *Front. Cell Dev. Biol.* **9**, 723804. doi:10.3389/fcell.2021.723804

Yu, T., Guo, W., Tian, Y., Xu, J., Chen, J., Li, L. and Wen, Z. (2017). Distinct regulatory networks control the development of macrophages of different origins in zebrafish. *Blood* **129**, 509-519. doi:10.1182/blood-2016-07-727651

Zelante, T. and Ricciardi-Castagnoli, P. (2012). The yin-yang nature of CSF1R-binding cytokines. *Nat. Immunol.* **13**, 717-719. doi:10.1038/ni.2375

Zhan, Y., Huang, Y., Chen, J., Cao, Z., He, J., Zhang, J., Huang, H., Ruan, H., Luo, L. and Li, L. (2018). Caudal dorsal artery generates hematopoietic stem and progenitor cells via the endothelial-to-hematopoietic transition in zebrafish. *J. Genet. Genomics* **45**, 315-324. doi:10.1016/j.jgg.2018.02.010

Zhang, C. C. and Lodish, H. F. (2004). Insulin-like growth factor 2 expressed in a novel fetal liver cell population is a growth factor for hematopoietic stem cells. *Blood* **103**, 2513-2521. doi:10.1182/blood-2003-08-2955

Zhang, Y., Jin, H., Li, L., Qin, F. X.-F. and Wen, Z. (2011). cMyb regulates hematopoietic stem/progenitor cell mobilization during zebrafish hematopoiesis. *Blood* **118**, 4093-4101. doi:10.1182/blood-2011-03-342501

Zhang, C., Patient, R. and Liu, F. (2013). Hematopoietic stem cell development and regulatory signaling in zebrafish. *Biochim. Biophys. Acta General Subjects* **1830**, 2370-2374. doi:10.1016/j.bbagen.2012.06.008

Zhang, P., He, Q., Chen, D., Liu, W., Wang, L., Zhang, C., Ma, D., Li, W., Liu, B. and Liu, F. (2015). G protein-coupled receptor 183 facilitates endothelial-to-hematopoietic transition via Notch1 inhibition. *Cell Res.* **25**, 1093-1107. doi:10.1038/cr.2015.109

Zriwil, A., Böiers, C., Wittmann, L., Green, J. C. A., Woll, P. S., Jacobsen, S. E. W. and Sitnicka, E. (2016). Macrophage colony-stimulating factor receptor marks and regulates a fetal myeloid-primed B-cell progenitor in mice. *Blood* **128**, 217-226. doi:10.1182/blood-2016-01-693887

Fig. S1

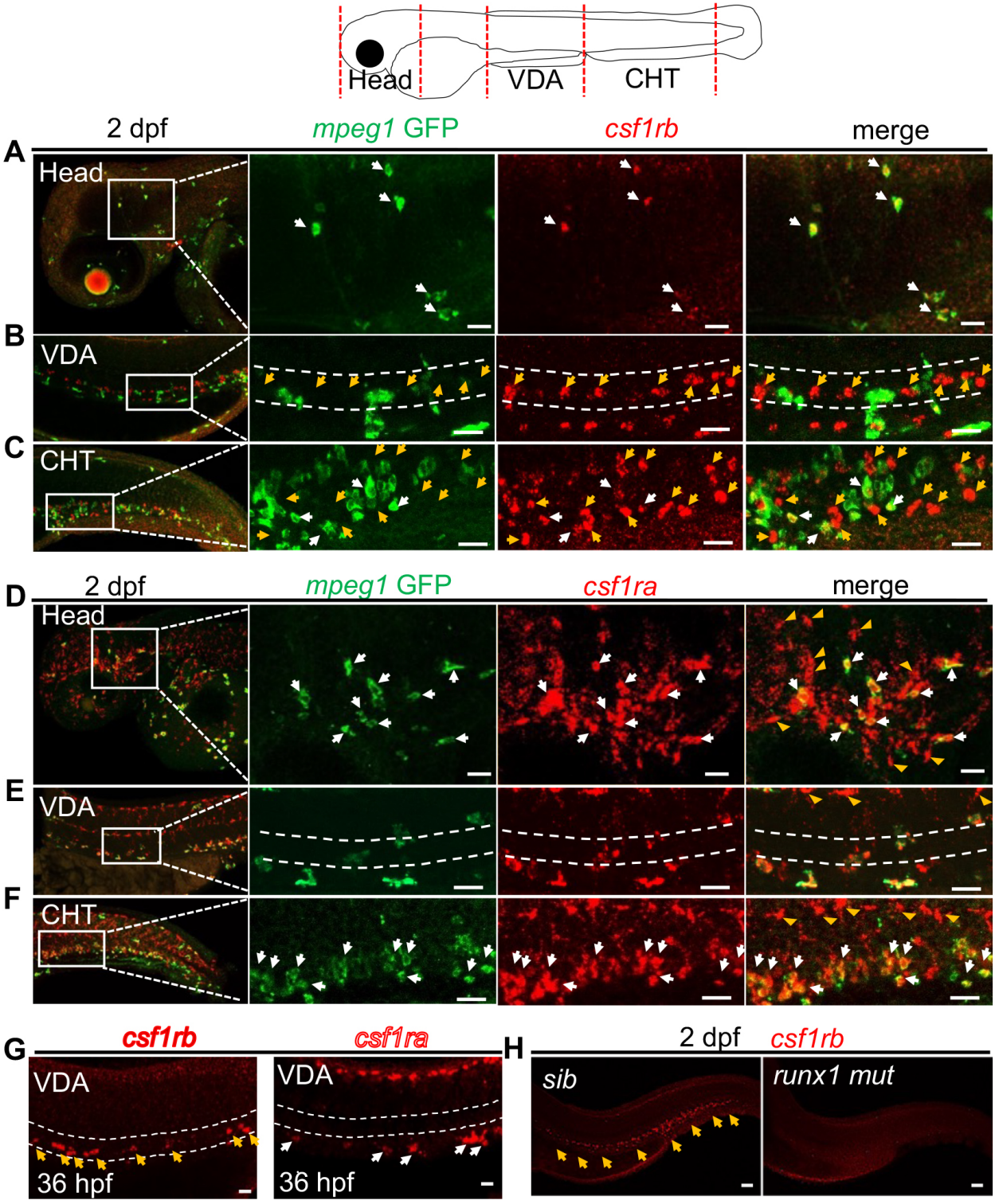

Fig. S1. Expression of *csf1ra/csf1rb* in zebrafish embryos.

Diagram indicates the imaging region: the head, the VDA, and the CHT. **A-C.** WISH of *csf1rb* in the *Tg(mpeg1:GFP)* at 2 dpf. **A,** Head region; **B,** the VDA region; **C,** the CHT region. The white rectangle indicates the position zoomed in; the White dashed line indicates the VDA region. The white arrow indicates co-localization of *csf1rb* (red) and GFP^+ macrophages (green). The yellow arrow indicates *csf1rb* single positive signal. Scale bars, 20 μm. **D-F.** WISH of *csf1ra* in the *Tg(mpeg1:GFP)* at 2 dpf. **D,** Head region; **E,** the VDA region; **F,** the CHT region. The white rectangle indicates the position zoomed in; the White dashed line indicates the VDA region. The white arrow indicates co-localization of *csf1ra* (red) and GFP^+ macrophages (green). The yellow triangle indicates *csf1ra* single positive xanthophore cells. Scale bars, 20 μm. **G.** WISH of *csf1rb* and *csf1ra* at 36 hpf, White dashed line indicates the VDA region; Yellow arrow indicates $csf1rb^+$ HSPCs signal. White arrow indicates $csf1ra^+$ macrophage signal; Scale bars, 20 μm. **H.** WISH of *csf1rb* at 2 dpf in *runx1* mutant, n (*sib*) = 52, n (*mut*) = 18; The yellow arrow indicates HSPCs signal. Scale bars, 50 μm.

Fig. S2

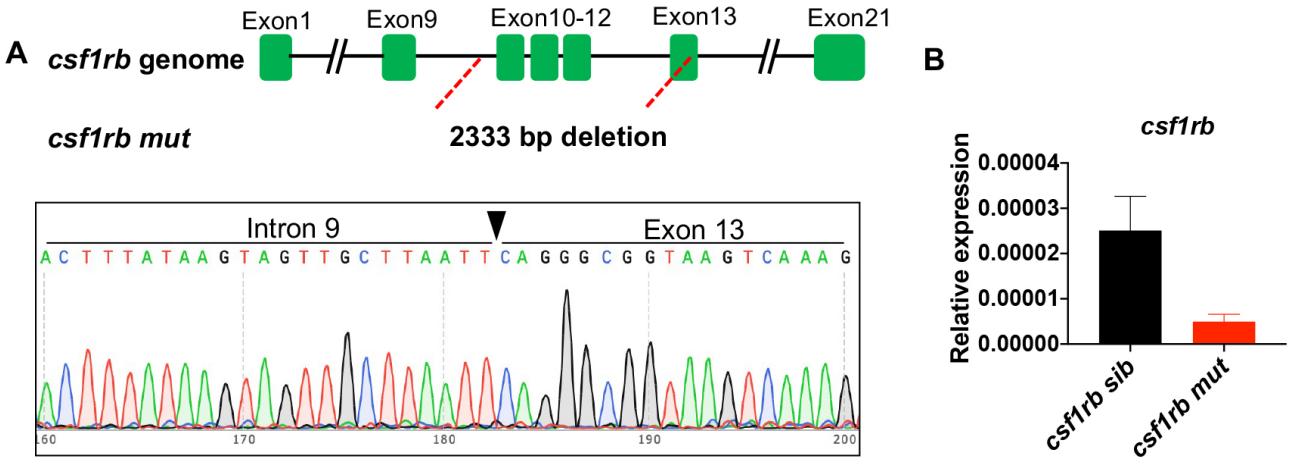

Fig. S2. characterization of *csf1rb* mutant. A. Diagram of *csf1rb* mutation. Mutant *csf1rb* genome harbors a 2333 bp deletion from intron 9 to exon 13, creating a pre-stop codon at exon14 in mutant *csf1rb* mRNA. The black triangle indicates the joint position of intron 9 and exon13 in mutant *csf1rb* genome. **B.** Relative expression level of *csf1rb* in *csf1rb* sibling and mutant embryos. Bars represent mean ± s.e.m. of 3 biological replicates.

Fig. S3

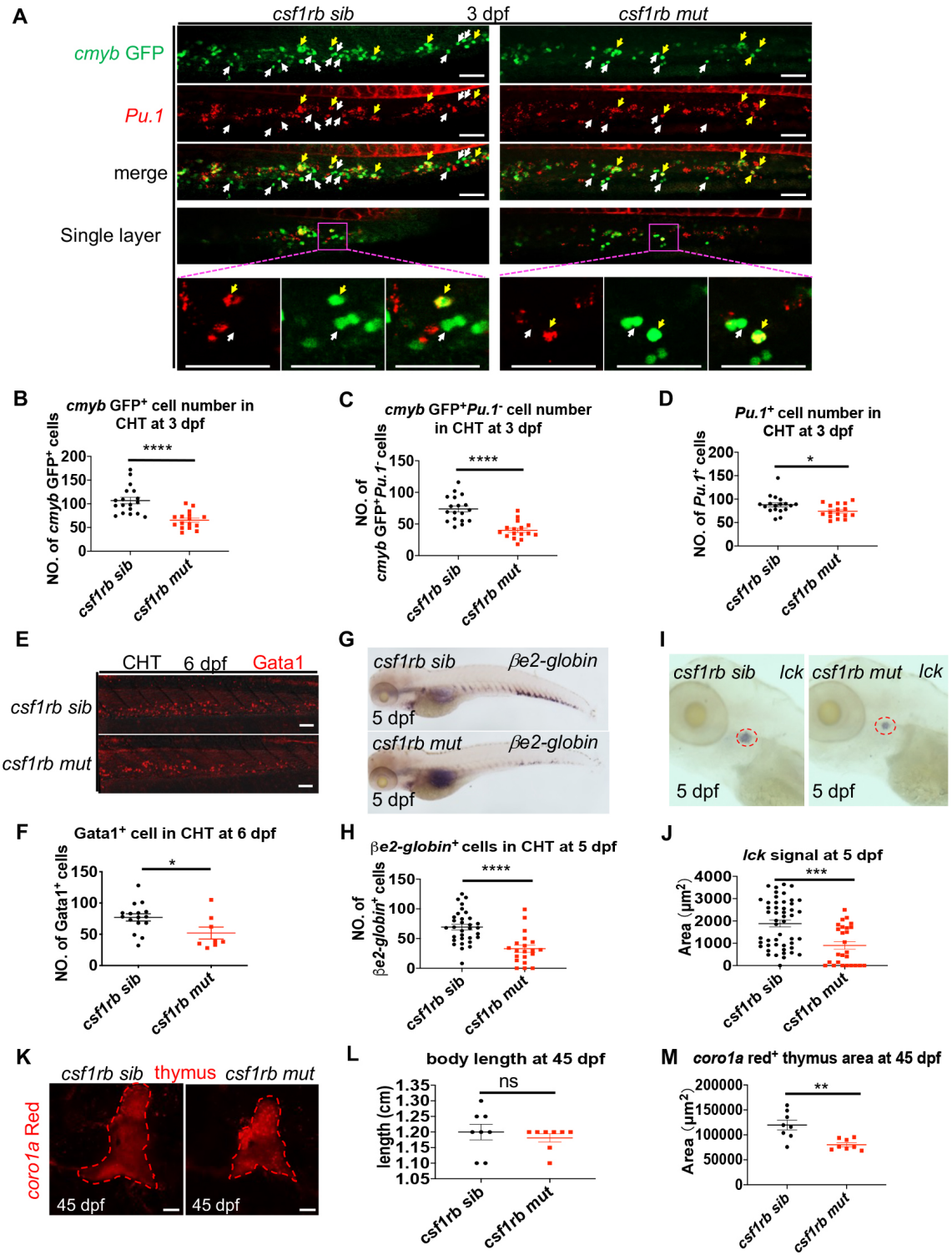

Fig. S3. HSPC and mature blood lineages defects in *csf1rb* mutant

A. WISH of *pu.1* in the *Tg(cmyb:GFP)* at 3 dpf in the CHT region. The yellow arrow indicates co-localization of *pu.1* (red) and GFP (green). The white arrow indicates GFP single positive HSPC. The magenta square shows the enlarged region of a single Z layer, demonstrating *pu.1*/ GFP double positive cells and GFP single positive cells. Scale bars, 50 μm**. B.** Quantification of *cmyb*-GFP positive total cells in the CHT region of *csf1rb* siblings (n=18) and *csf1rb* mutants (n=16). **C.** Quantification of *cmyb*-GFP^{+}*pu.1*$^{-}$ cells in the CHT region of *csf1rb* siblings (n=18) and *csf1rb* mutants (n=16). **D.** Quantification of *pu.1* positive cell in the CHT region of *csf1rb* siblings (n=18) and *csf1rb* mutants (n=16). **E.** Immunostaining of Gata1 in the CHT at 6 dpf in siblings and *csf1rb* mutants. Scale bars, 50 μm. **F.** Quantification of the Gata1^{+} erythroid progenitor cells in siblings (n=16) and *csf1rb* mutant embryos (n=8). **G**. WISH of *βe2-globin* at 5 dpf in siblings and *csf1rb* mutants. **H.** Quantification of *βe2-globin*$^{+}$ cells in the CHT at 5 dpf in siblings (n=32) and *csf1rb* mutants (n=20). **I**. WISH of *lck* at 5 dpf in siblings and *csf1rb* mutants. **J.** Quantification of *lck*$^{+}$ thymus area at 5 dpf in siblings (n=49) and *csf1rb* mutants (n=26). **K.** *Coro1a*-DsRedx^{+} T cell signal in the thymus at 45 dpf in siblings and *csf1rb* mutants. Scale bars, 100 μm. **L.** Body length of siblings (n=8) and *csf1rb* mutants (n=8) at 45 dpf. **M.** Quantification of *coro1a*$^{+}$ thymus area at 45 dpf in siblings (n=8) and *csf1rb* mutants (n=8). Data are presented as mean ± s.e.m. *$p < 0.05$, **$p < 0.01$, ***$p < 0.001$, ****$p < 0.0001$; ns, not significant.

Fig. S4

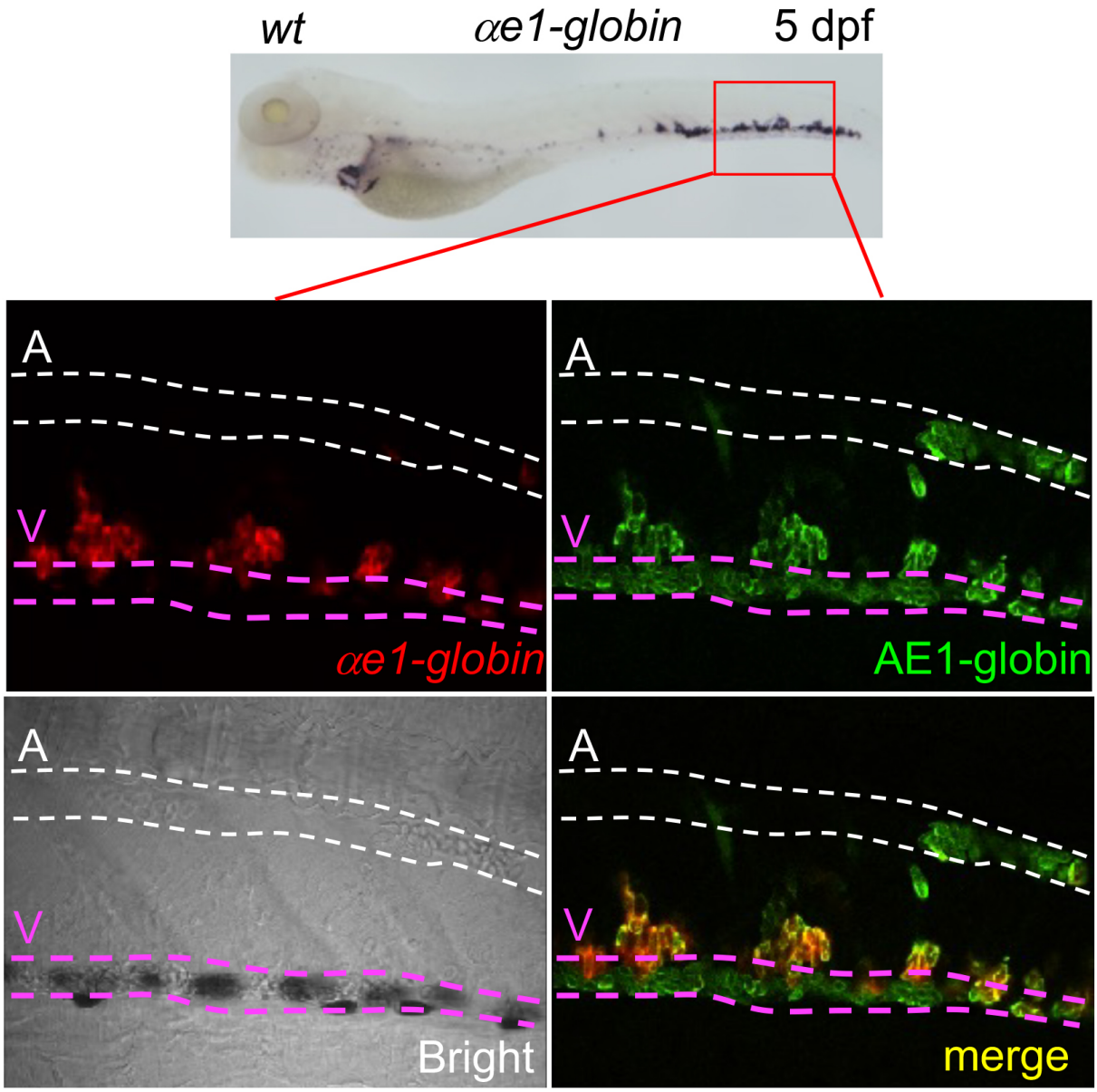

Fig. S4. Immunostaining of *αe1-globin* RNA and AE1-globin protein at 5 dpf.

αe1-globin RNA (red) was mainly detected in the CHT with occasionally occurrence in the circulation. AE1-globin protein (green) retained in erythroid cells from both the circulation and the CHT. A, artery, white dashed line; V, vein, magenta dashed line.

Fig. S5

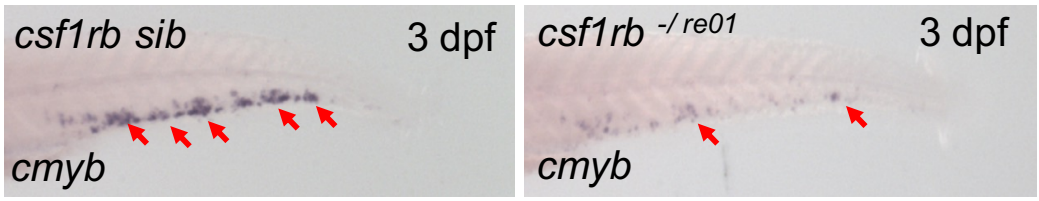

Fig. S5. Hematopoietic defects in *csf1rb*$^{-/re01}$ mutants. WISH of *cmyb* at 3 dpf in siblings (n = 21) and *csf1rb*$^{-/re01}$ mutants (n = 18). Red arrows indicate *cmyb*$^{+}$ HSPCs.

Fig. S6

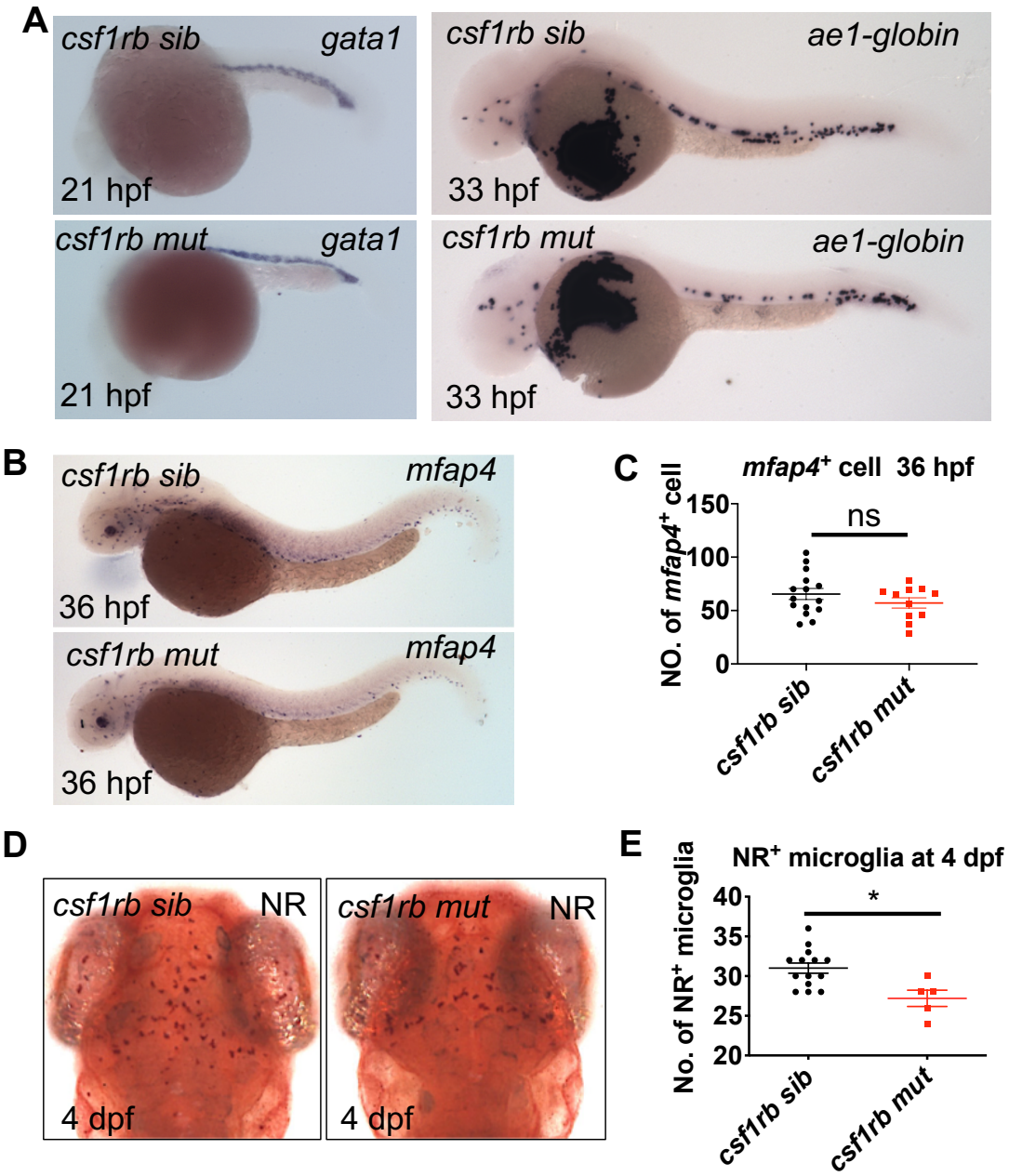

Fig. S6. Primitive erythroid and myeloid development in siblings and *csf1rb* mutants.

A. WISH of *gata1* at 21 hpf and *ae1-globin* at 33 hpf in siblings (n_{gata1} = 13, n_{ae1} = 24) and *csf1rb* mutants (n_{gata1} = 13, n_{ae1} = 8). **B.** WISH of *mfap4* at 36 hpf in siblings and *csf1rb* mutants. **C.** Quantification of the *mfap4*$^+$ myeloid cells of siblings (n=15) and *csf1rb* mutant embryos (n=11). **D.** Neutral red (NR) staining at 4 dpf in siblings and *csf1rb* mutants. **E.** Quantification of the NR$^+$ microglia in the brain of siblings (n=14) and *csf1rb* mutant embryos (n=5). Data are presented as mean ± s.e.m. *$p < 0.05$, ns, not significant.

Fig. S7

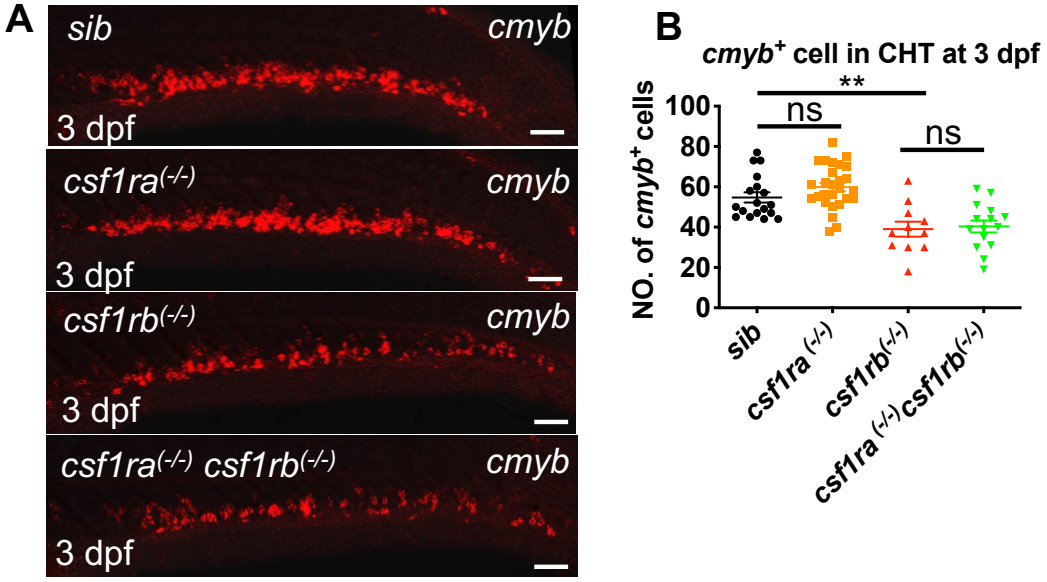

Fig. S7. HSPCs defects in *csf1ra* and *csf1rb* mutants.

A. WISH of *cmyb* in siblings, *csf1ra/csf1rb* single or double mutants at 3 dpf. Scale bars, 50 μm. **B.** Quantification of *cmyb*$^{+}$ HSPCs in the CHT at 3 dpf in siblings and *csf1ra/csf1rb* single or double mutants. n ($csf1rb_{sib}$ + $csf1ra_{mut}$ + $csf1rb_{mut}$ + $csf1ra_{mut}csf1rb_{mut}$) = n (18 + 27 +11 + 15). Data are presented as mean ± s.e.m. $^{**}p < 0.01$. ns, not significant.

Fig. S8

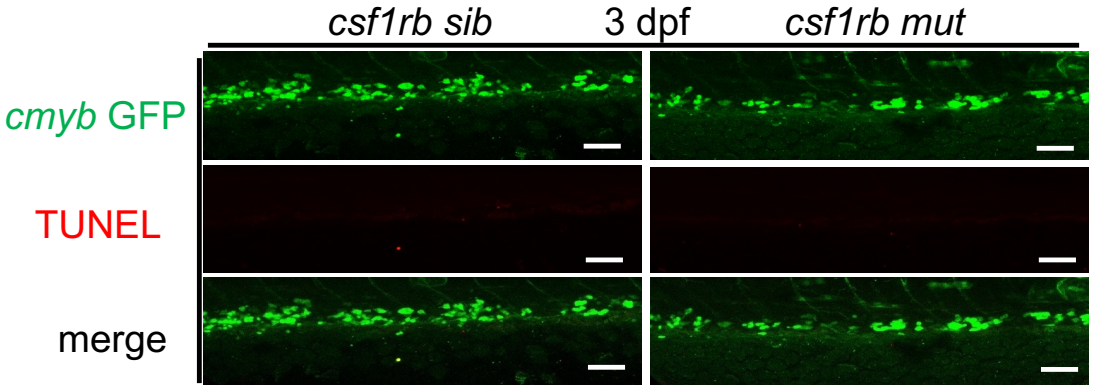

Fig. S8. No cell death of HSPCs is detected in *csf1rb* mutants.

TUNEL assay in the CHT at 3 dpf in siblings (n=53) and *csf1rb* mutants (n=16). TUNEL is shown with red color. *cmyb*-GFP^{+} HSPCs are indicated with green color. Scale bars, 50 μm.

Fig. S9

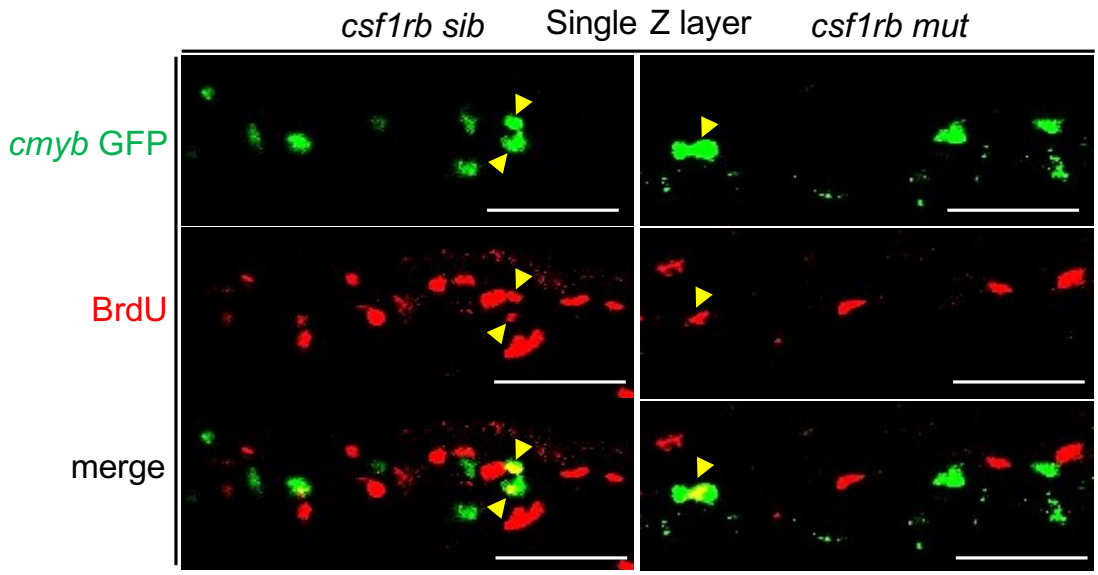

Fig. S9. Demonstration of co-localization of BrdU and *cmyb*-GFP in *csf1rb* siblings and mutants within single layer images.

Yellow arrow heads indicate Brdu (red) and GFP (green) double positive HSPCs. Scale bars, 50 μm.

Fig. S10

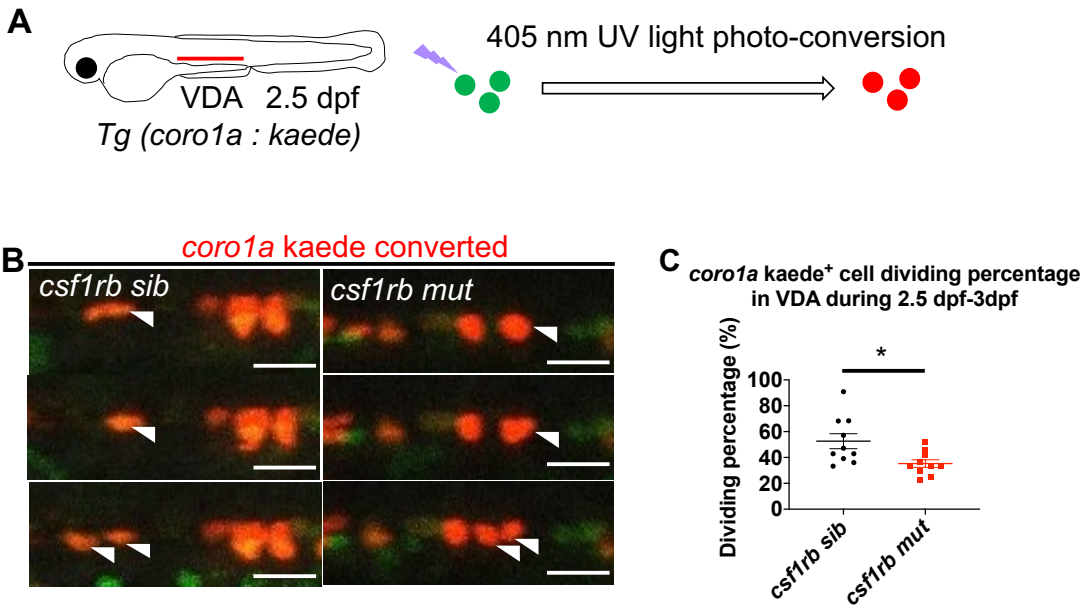

Fig. S10. *Csf1rb* deficiency impairs the proliferation capacity of *coro1a*$^+$ HSPC/ hematopoietic cells in the VDA. A. Diagram of photo-conversion of *coro1a*- kaede$^+$ cells in the VDA. The Red line indicates the VDA region. Kaede$^+$ cells are shown in green color, after UV light conversion, cells are labeled in red color in the VDA. **B.** Conversion of *coro1a*-Kaede$^+$ cells in the VDA at 2.5 pdf in both siblings and *csf1rb* mutants. The Left and right panels show the dividing *coro1a*$^+$ cells in sibling and mutant, respectively. White triangles indicate the cell undergoes division. Scale bars, 20 μm. **C.** Dividing percentage of converted *coro1a*$^+$ cells in the VDA from 2.5 dpf to 3dpf in siblings (n=10) and *csf1rb* mutants (n=10). Data are presented as mean ± s.e.m. *$p < 0.05$

Fig. S11

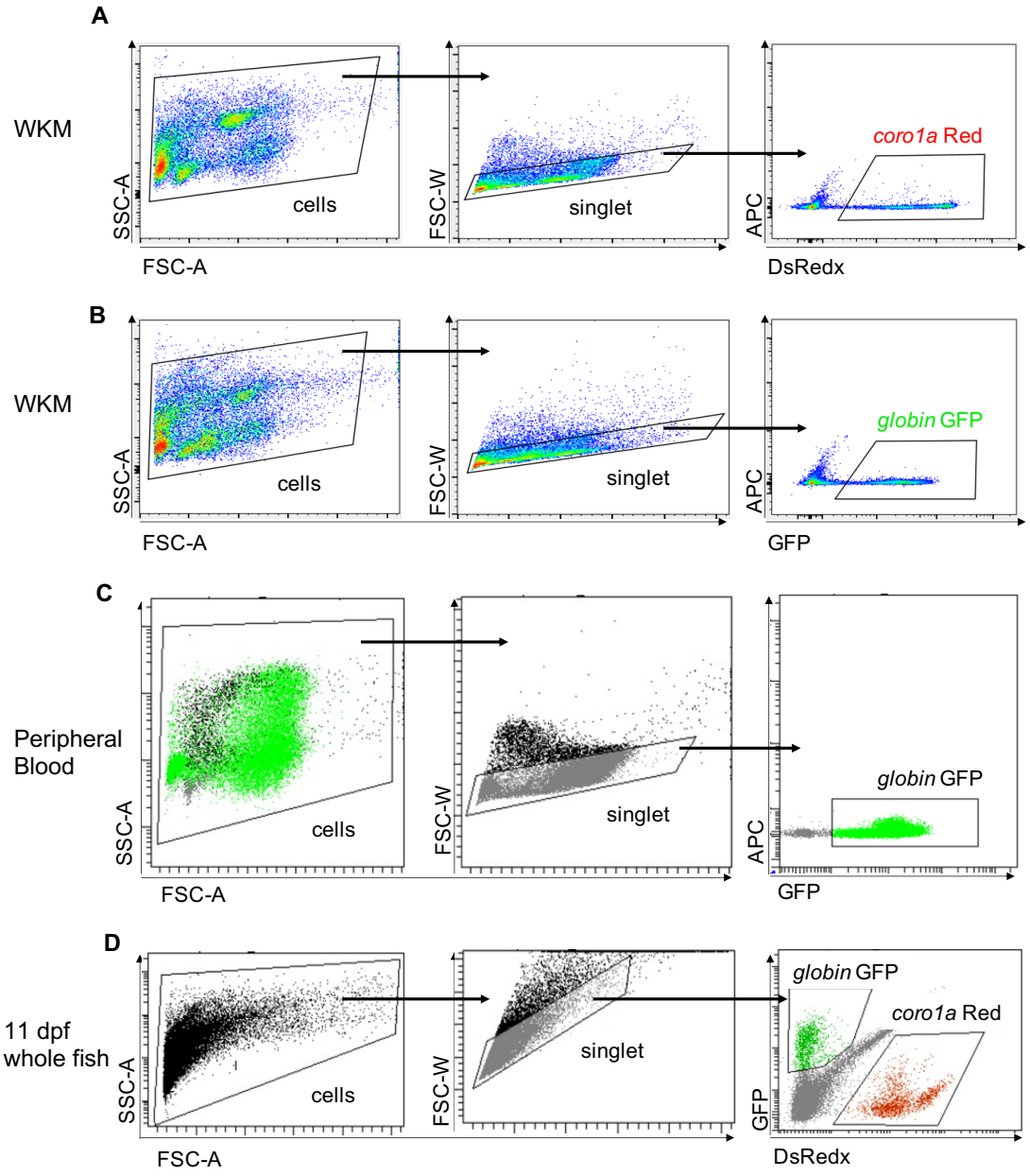

Fig. S11. Gating strategies of flow cytometry.

A. Gating strategies of flow cytometry of the adult whole kidney marrow cells (WKM) with *coro1a*-DsRedx^{+} cells. **B.** Gating strategies of flow cytometry of the adult WKM with *globin*-GFP^{+} cells. **C.** Gating strategies of flow cytometry of adult peripheral blood with *globin*-GFP^{+} cells. **D.** Gating strategies of flow cytometry of 11 dpf whole fishes with *coro1a*-DsRedx^{+} cells and *globin*-GFP^{+} cells.

Fig. S12

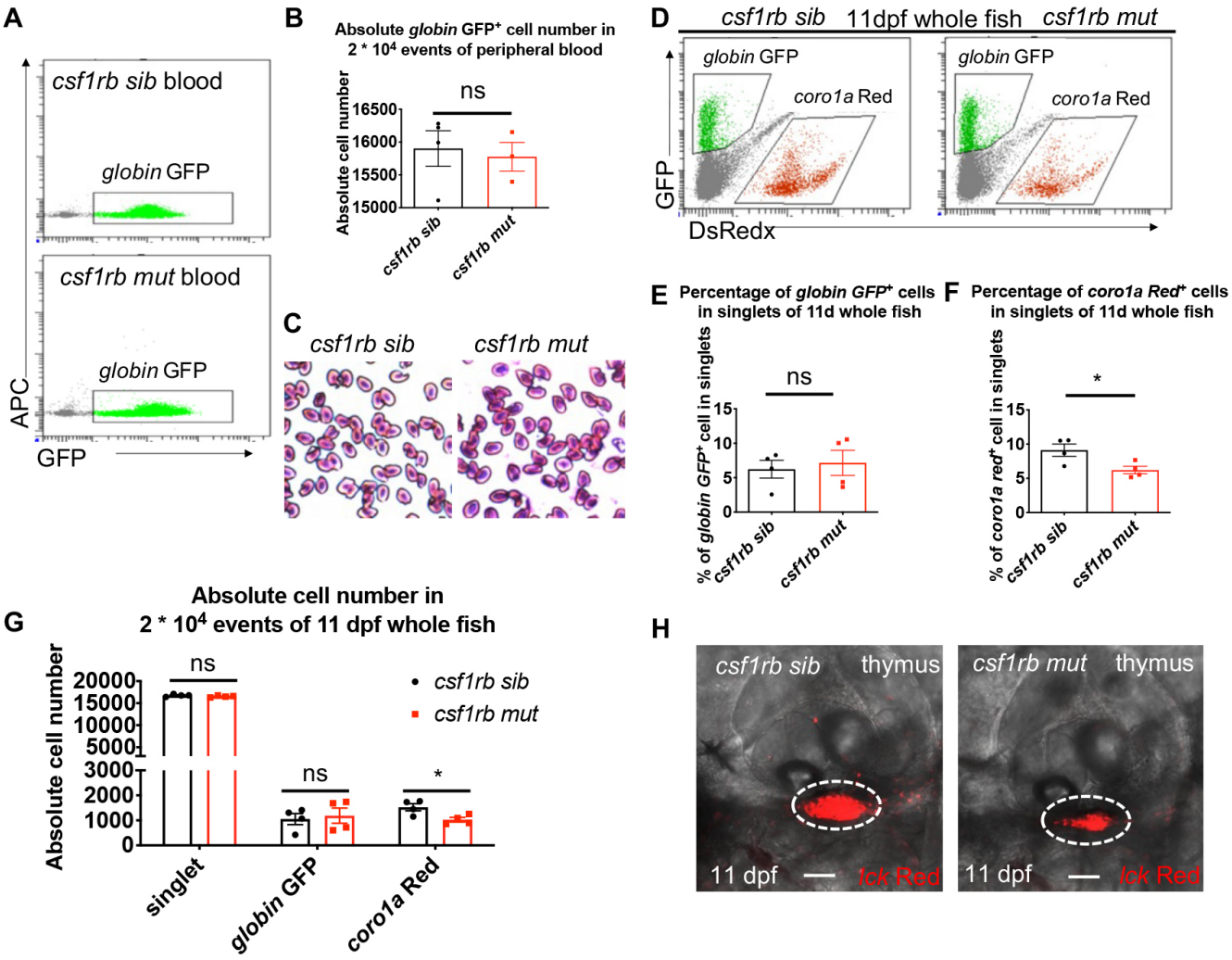

Fig. S12. Normal Erythroid population in peripheral blood of adult *csf1rb* mutant and erythroid defects recover in juvenile *csf1rb* mutant.

A. Flow cytometry file of peripheral blood of adult siblings and *csf1rb* mutants within the *Tg(globin: GFP),* labeling mature erythroid cells. **B.** Absolute cell number of *globin*-GFP^{+} erythroid cells in 2*10^{4} cell events of adult peripheral blood in siblings (n=4) and *csf1rb* mutants (n=3). **C.** May-Grunwald and Giemsa staining of adult peripheral blood in siblings and *csf1rb* mutants, top, siblings, bottom, mutants. **D.** Flow cytometry file of 11 dpf whole fish of siblings and *csf1rb* mutants within the *Tg(globin:GFP)* and *Tg(coro1a: DsRedx)*, labeling mature erythroid cells and leukocytes/ progenitors, respectively. **E.** Percentage of *globin*-GFP^{+} erythroid cells in singlets of whole fish in 11 dpf siblings (n=4) and *csf1rb* mutants (n=4). **F.** Percentage of *coro1a*-DsRedx^{+} progenitors/ leukocytes in singlets of whole fish in 11 dpf siblings (n=4) and *csf1rb* mutants (n=4). **G.** Absolute cell number of *coro1a*-DsRedx^{+} cells and *globin*-GFP^{+} erythroid cells in 2*10^{4} events of whole fish in 11 dpf siblings (n=4) and *csf1rb* mutants (n=4). **E-G**, each dot represents 2 juveniles pooled. **H.** *lck*-DsRedx^{+} T cells in the thymus in 11 dpf siblings (n=11) and *csf1rb* mutants (n=10), white dashed line indicates the thymus region. Scale bars, 50 μm. Data are presented as mean ± s.e.m. *$p < 0.05$. ns, not significant.

Fig. S13

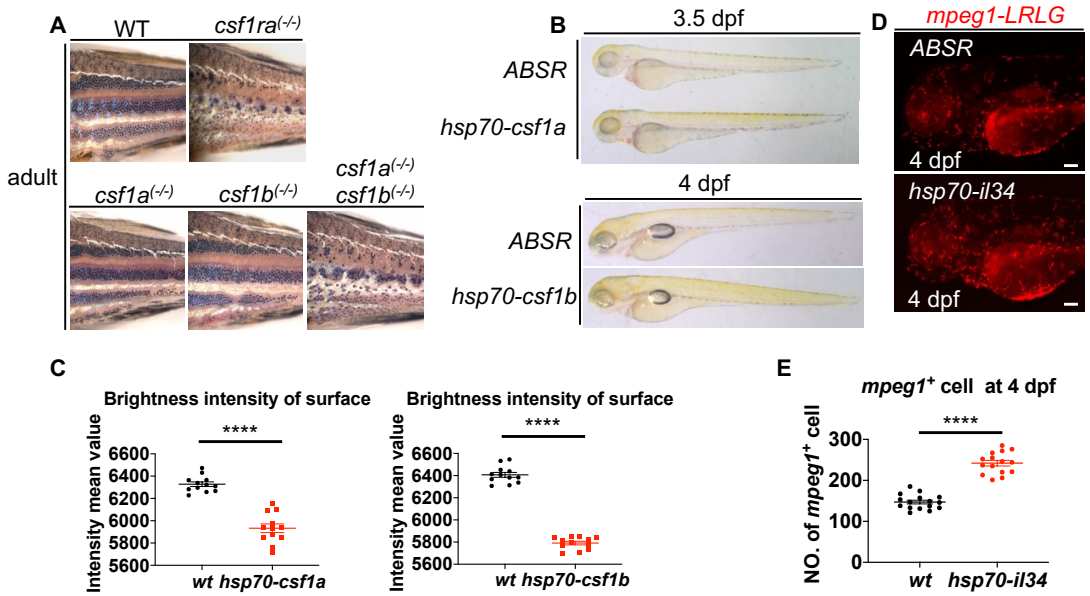

Fig. S13. Loss of function and gain of function of ligands.
A. Double deficiency of *csf1a* and *csf1b* recapitulates pigment defects of *csf1ra* mutant fish at adulthood, suggesting that mutations of Csf1 ligands lead to complete loss of protein functions. **B.** Ectopic expression of *csf1a* or *csf1b* increases xanthophore cells (yellow), suggesting functional overexpression of ligands. **C.** Quantification of surface brightness intensity of *wt* fish and fish with ectopic expression of *csf1a* or *csf1b*. **D.** Ectopic expression of *il34* increases *mpeg1*$^{+}$ macrophages, suggesting functional overexpression of ligand. Scale bars, 100 µm. **E.** Quantification of *mpeg1*$^{+}$ macrophages in the imaged region of *wt* fish and fish with ectopic expression of *il34*. Data are presented as mean ± s.e.m. ****$p < 0.0001$. ns, not significant.

Fig. S14

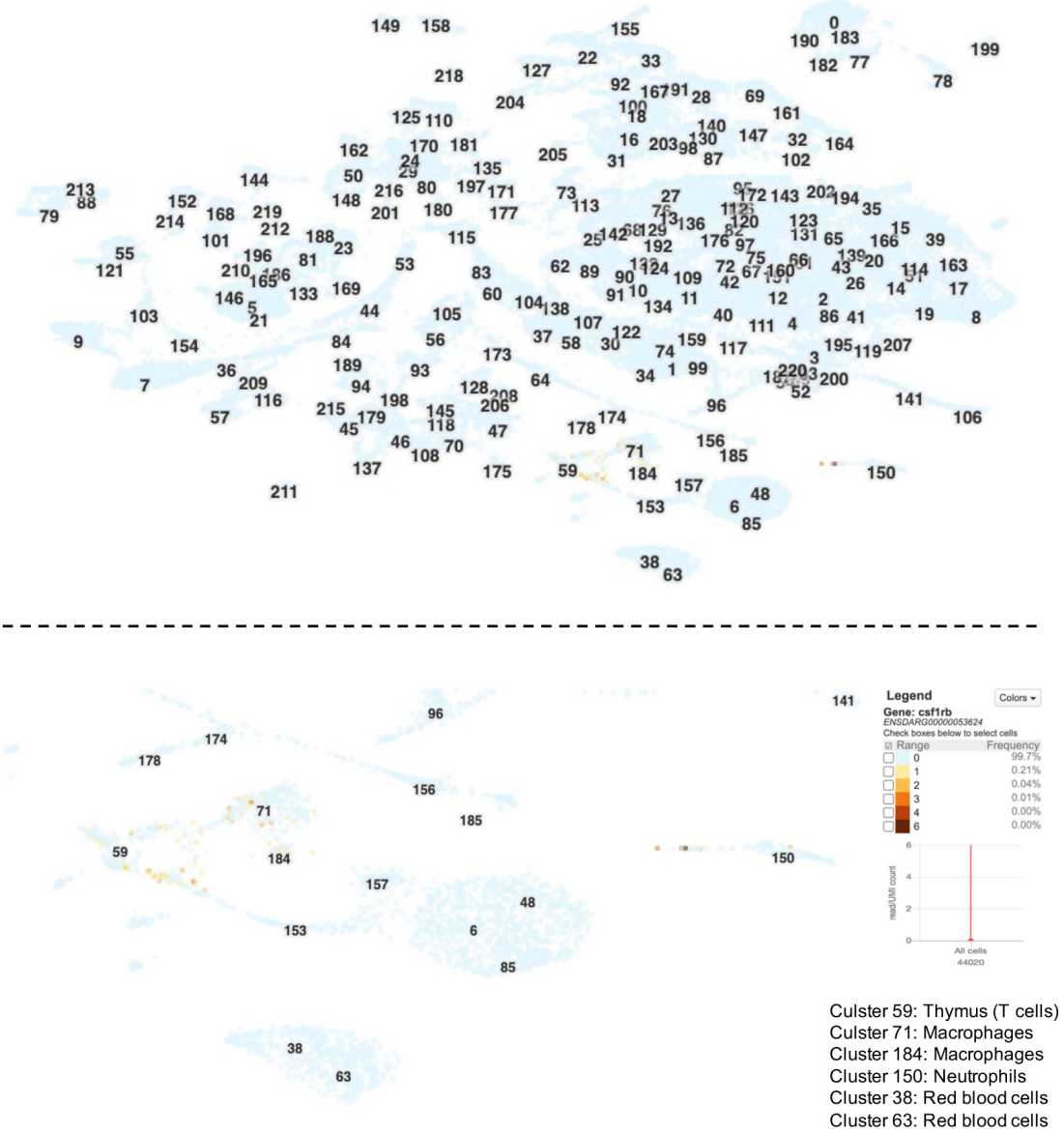

Fig. S14. Relative expression of *csf1rb* in the UCSC Cell Browser with Atlas for Zebrafish Development Dataset.

Upper panel, cell type clusters from Single-cell RNA-seq data of 1 dpf, 2 dpf, and 5 dpf zebrafish embryos are defined and numbered in the UCSC Cell Browser. Bottom panel, clusters of T cells, myeloid cells, and erythrocytes are enlarged to show the relative expression of *csf1rb*. Expression of *csf1rb* were detected in T cells of the thymus (cluster 59) and myeloid cells (cluster 71, cluster 184, and cluster 150), but not in erythrocytes (cluster 38 and cluster 63).

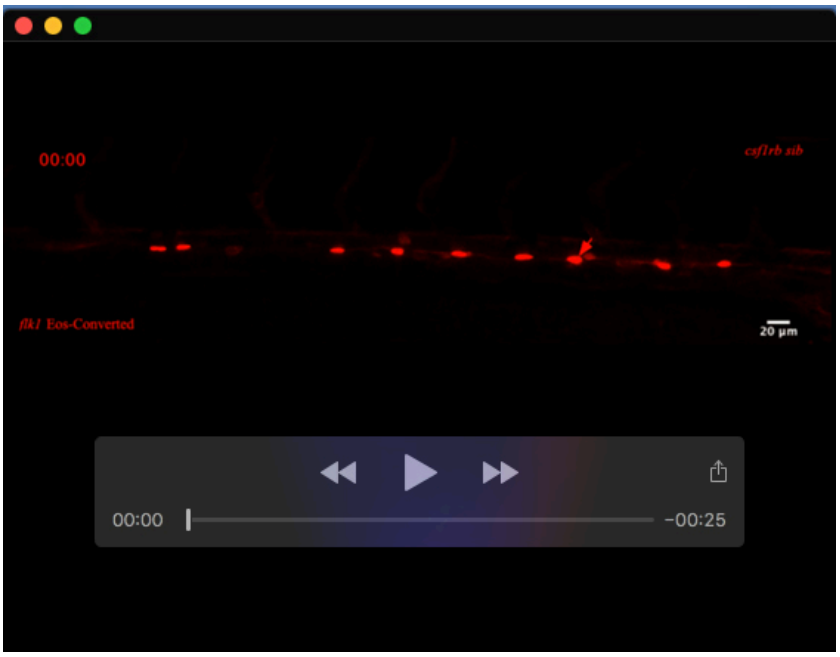

Movie 1. EHT process in *csf1rb* sibling.
Time-Lapse imaging of converted *flk1*-Eos^{+} endothelial cells (Red^{+}) in the VDA region from 30 hpf right after conversion in *csf1rb* siblings. The red arrow indicates the cell undergo EHT during imaging. Time scale (min: sec) indicates the time starting from live imaging.

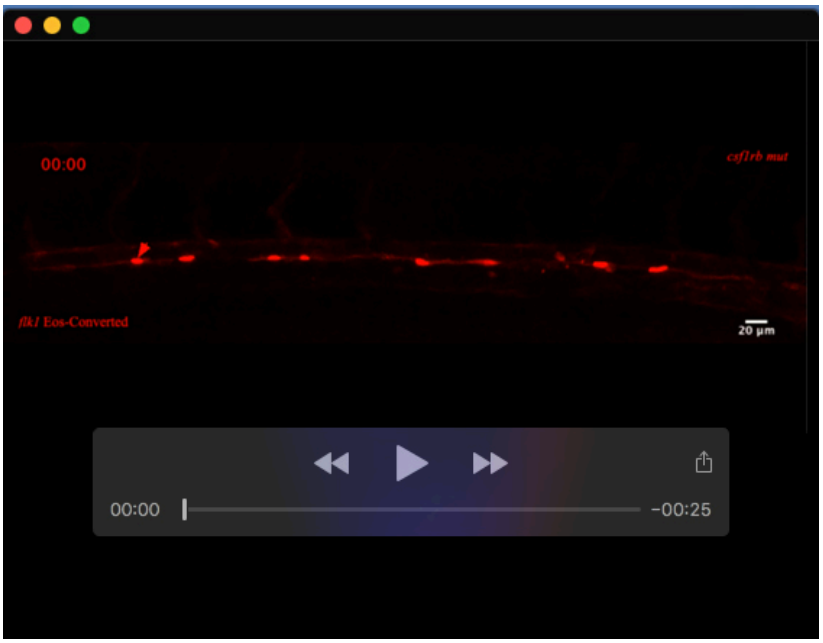

Movie 2. EHT process in *csf1rb* mutant.
Time-Lapse imaging of converted *flk1*-Eos^{+} endothelial cells (Red^{+}) in the VDA region from hpf right after conversion in *csf1rb* mutants. The red arrow indicates the cell undergo EHT during imaging. Time scale (min: sec) indicates the time starting from live imaging.

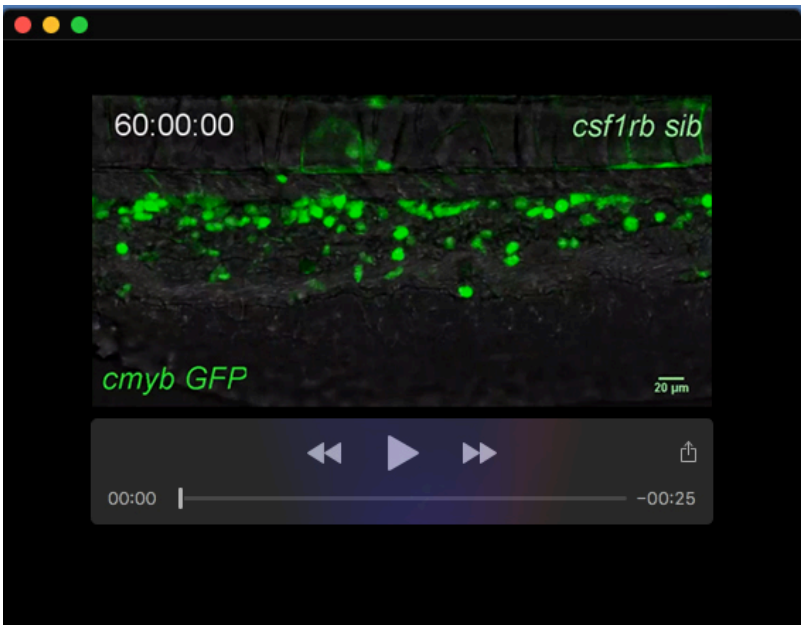

Movie 3. Time-Lapse imaging of HSPCs in *csf1rb* sibling.
Time-Lapse imaging of *cmyb*-GFP^{+} HSPCs in the CHT region from 60-86 hpf in *csf1rb* siblings. Time scale (hr: min: sec) indicates the time starting from the development stage.

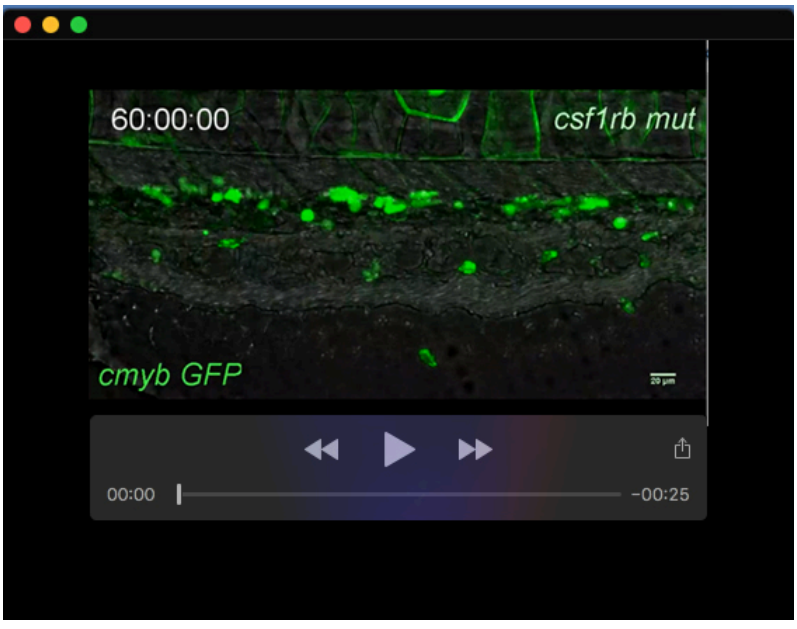

Movie 4. Time-Lapse imaging of HSPCs in *csf1rb* mutant.
Time-Lapse imaging of *cmyb*-GFP^{+} HSPCs in the CHT region from 60-86 hpf in *csf1rb* mutants. Time scale (hr: min: sec) indicates the time starting from the development stage.